12-15-2007

Energy Storage System Requirements For Shipboard Power Systems Supplying Pulsed Power Loads

Prashanth Duvoor

ENERGY STORAGE SYSTEM REQUIREMENTS FOR SHIPBOARD POWER SYSTEMS SUPPLYING PULSED POWER LOADS

By

Prashanth Duvoor

A Thesis
Submitted to the Faculty of
Mississippi State University
in Partial Fulfillment of the Requirements
for the Degree of Master of Science
in Electrical Engineering
in the Department of Electrical and Computer Engineering

Mississippi State, Mississippi

December 2007

ENERGY STORAGE SYSTEM REQUIREMENTS FOR SHIPBOARD POWER SYSTEMS SUPPLYING PULSED POWER LOADS

By

Prashanth Duvoor

Approved:

Herbert L. Ginn III Assistant Professor of Electrical and Computer Engineering (Major Advisor and Director of Thesis)	Noel N. Schulz Associate Professor of Electrical and Computer Engineering (Committee Member)
Anurag K. Srivastava Assistant Professor of Electrical and Computer Engineering (Committee Member)	Nicholas H. Younan Professor of Electrical and Computer Engineering (Graduate Coordinator)
Roger King Associate Dean of College of Engineering	

Name: Prashanth Duvoor

Date of Degree: December 14, 2007

Institution: Mississippi State University

Major Field: Electrical and Computer Engineering

Major Professor: Dr. Herbert L. Ginn III

Title of Study: ENERGY STORAGE SYSTEM REQUIREMENTS FOR SHIPBOARD POWER SYSTEMS SUPPLYING PULSED POWER LOADS

Pages in Study: 83

Candidate for Degree of Master of Science

Energy storage systems will likely be needed for future shipboard power systems that supply loads with high power variability such as pulsed power loads. Two fundamental items in evaluating the requirements of an energy storage system are the energy storage capacity and the ratings of the power conversion equipment that interfaces the energy device to the power system. The supply current of pulsed power load systems is aperiodic and cannot be described in terms of active power. Therefore traditional methods of rating power equipment cannot be used. This thesis describes an approach to determine the ratings of an energy storage interface and the energy storage capacity as a function of load and supply parameters. The results obtained using the proposed approach are validated with the results obtained from the simulation model of the generator supplying a pulsed power load in conjunction with an energy storage system.

DEDICATION

I would like to dedicate this research work to my parents.

ACKNOWLEDGMENTS

I would like to express my gratitude to my advisor Dr. Herbert L. Ginn III for his support, guidance, and encouragement throughout this research. I would also like to extend my thanks to the other committee members, Dr. Noel N. Schulz and Dr. Anurag K. Srivastava for serving on my committee to improve this work. I am grateful to Dr. Noel N. Schulz for her invaluable support during the summer of 2006. I would like to specially thank Dr. Robert E. Hebner and Dr. Hamid Ouroua of Center for Electromechanics in University of Texas, Austin.

I would like to thank the Office of Naval Research (ONR) for financial support for this project.

I would also like to thank my friends Sundar and Konstantin Borisov for their help.

TABLE OF CONTENTS

Page

DEDICATION ii

ACKNOWLEDGMENTS iii

LIST OF TABLES vi

LIST OF FIGURES viii

I. INTRODUCTION 1

1.1 Introduction 1
1.2 Objective of this Research Work 2
1.3 Thesis Overview 3
1.4 Thesis Organization 4

II. DESCRIPTION OF THE ALL ELECTRIC SHIP 6

2.1 Concept of the All Electric Ship 6
2.2 IPS Architecture in Future Ship Board Power Systems 8
2.2.1 US Navy Integrated Power System Test Facility 8
2.2.2 ONR Reference System 10
2.2.3 Notional DD (X) Power System for Future Shipboard Power Systems 11
2.3 Pulsed Power Loads in Shipboard Power Systems 13
2.4 Energy Management for Shipboard Power Systems 18

III. ANALYSIS OF APERIODIC CURRENTS IN SHIPBOARD POWER SYSTEM 21

3.1 Signal Processing in Power Electronic Applications 21
3.1.1 Fourier Series 21

3.1.2 Properties of Pulsed Power Load System Supply Currents 23
3.1.3 Moving Window Discrete Fourier Transform 24
3.2 Current Physical Components' Power Theory 26
3.3 Load Current Decomposition for a Power System with Pulsed Power Load 29

IV. DETERMINATION OF THE RATINGS OF ENERGY STORAGE SYSTEMS 35

4.1 Modeling of a Pulsed Power Load System 35
4.2 Pulsed Power Load System Compensators 37
4.3 Supply Side Effects of Pulsed Power Load Systems 39
4.4 Minimization of Power Loss on the DC Bus of the Pulsed Power Load System 49
4.4.1 Solving the Optimization Problem 51
4.5 Ratings of an Energy Storage System Operating in Conjunction with the Main Generator 51

V. TEST CASE AND RESULTS 54

5.1 Simulation Tool to Analyze the Effects of Pulsed Power Load System Compensation 54
5.2 Simulation Case Study 56
5.3 Analytical Tool to Analyze the Effects of Pulsed Power Load System Compensation 60
5.4 Numerical Tests 63

VI. CONCLUSIONS 66

REFERENCES 68

APPENDIX

A. ENERGY STORAGE SYSTEM RATINGS (80 MW/10 kV) 70

B. ENERGY STORAGE SYSTEM RATINGS (80 MW/5 kV) 77

LIST OF TABLES

TABLE Page

5.1 Comparison Between Simulation Tool and Analytical Tool 62

A.1 Energy Storage Ratings for 100 MJ Pulse (80 MW/10 kV)..... 71

A.2 Energy Storage Ratings for 110 MJ Pulse (80 MW/10 kV)..... 71

A.3 Energy Storage Ratings for 120 MJ Pulse (80 MW/10 kV)..... 72

A.4 Energy Storage Ratings for 130 MJ Pulse (80 MW/10 kV)..... 72

A.5 Energy Storage Ratings for 140 MJ Pulse (80 MW/10 kV)..... 73

A.6 Energy Storage Ratings for 150 MJ Pulse (80 MW/10 kV)..... 73

A.7 Energy Storage Ratings for 160 MJ Pulse (80 MW/10 kV)...…….. 74

A.8 Energy Storage Ratings for 170 MJ Pulse (80 MW/10 kV)..... 74

A.9 Energy Storage Ratings for 180 MJ Pulse (80 MW/10 kV)..... 75

A.10 Energy Storage Ratings for 190 MJ Pulse (80 MW/10 kV)..... 75

A.11 Energy Storage Ratings for 200 MJ Pulse (80 MW/10 kV)..... 76

B.1 Energy Storage Ratings for 100 MJ Pulse (80 MW/5 kV)..... 78

B.2 Energy Storage Ratings for 110 MJ Pulse (80 MW/5 kV)..... 78

B.3 Energy Storage Ratings for 120 MJ Pulse (80 MW/5 kV).....…….. 79

B.4 Energy Storage Ratings for 130 MJ Pulse (80 MW/5 kV)..... 79

B.5 Energy Storage Ratings for 140 MJ Pulse (80 MW/5 kV)..... 80

TABLE Page

B.6 Energy Storage Ratings for 150 MJ Pulse (80 MW/5 kV)..... 80

B.7 Energy Storage Ratings for 160 MJ Pulse (80 MW/5 kV)..... 81

B.8 Energy Storage Ratings for 170 MJ Pulse (80 MW/5 kV)..... 81

B.9 Energy Storage Ratings for 180 MJ Pulse (80 MW/5 kV)..... 82

B.10 Energy Storage Ratings for 190 MJ Pulse (80 MW/5 kV)……..…….. 82

B.11 Energy Storage Ratings for 200 MJ Pulse (80 MW/5 kV)..... 83

LIST OF FIGURES

FIGURE		Page
2.1	Electric Propulsion System	7
2.2	Integrated Propulsion System	8
2.3	US Navy Integrated Power System	9
2.4	Actual Setup of the US Navy Integrated Power System Test Facility [3]	9
2.5	ONR Reference System Configuration	10
2.6	Notional DD (X) Power System for Future Electric Ship [5]	12
2.7	Pulsed Power Load System	14
2.8	Pulsed Power Load Connected to the AC Side through a Diode Bridge, Inductor and a Capacitor	15
2.9	Pulsed Power Load Input Current	16
2.10	Pulsed Power Load System Supply Current and Input Current	16
2.11	Capacitor Voltage	17
2.12	Supply Current and Input Current of a Pulsed Power Load	17
2.13	A Future Combatant Electric Ship [6]	20
3.1	Illustration of Moving Window DFT	25
3.2	Three-Phase System with Linear Time-Invariant Load	26
3.3	Equivalent Load with respect to Active Power	27
3.4	Equivalent Load with respect to Reactive Power	28

FIGURE Page

3.5 Equivalent Delta-Connected Load 28

3.6 Active Current at the Fundamental Frequency with Phase Voltage 30

3.7 Reactive Current at the Fundamental Frequency with Phase Voltage 31

3.8 Unbalanced Current at the Fundamental Frequency with Phase Voltage 31

3.9 Distorted Current Waveform with Phase Voltage 32

4.1 Pulsed Power Load System Model in MATLAB/Simulink 36

4.2 Example DC Current at the Output Terminals of the Diode Bridge Rectifier 37

4.3 Structure of Compensators for Pulsed Power Load System 38

4.4 Series RLC Circuit 39

4.5 Series RLC Circuit Connected to a Three-Phase Diode Bridge Rectifier 42

4.6 Indication of the Measurement Location in Figure 4.5 43

4.7 Generator Supplying a Pulsed Power Load System 46

4.8 Example Plot of Capacitor Voltage during Pulsed Power Load Operation .. 47

5.1 Pulse Power Load System Model – Input Parameters 55

5.2 Running Load Active Power Over One Cycle of the Supply Voltage 57

5.3 Running Generator Active Power Over One Cycle of the Supply Voltage .. 58

5.4 Running Injected Active Power Over One Cycle of the Supply Voltage 58

5.5 RMS Value of the Injected Active Current over One Cycle of the Supply Voltage 59

5.6 DC Bus Voltage across the Capacitor 59

5.7 Input Current of the Pulsed Power Load 60

FIGURE Page

5.8 Pictorial Representation of the Analytical Tool used to Estimate the Ratings of the Energy Storage System 62

5.9 Current Ratings of Energy Storage Interface for 80 MW Generation Power and 10 kV Change in DC Bus Voltage 64

5.10 Current Ratings of Energy Storage Interface for 80 MW Generation Power and 5 kV Change in DC Bus Voltage 65

CHAPTER I

INTRODUCTION

1.1 Introduction

The ongoing research on energy storage systems for land, sea and space based power systems have intensified in the recent past. The main power sources in some cases may not be sufficient to satisfy the peak power load demand in a power system, which makes energy storage systems necessary. Energy storage systems act as compensators if the power demand is beyond the capacity of the generator(s). Pulsed power loads are high power loads that require energy in short intervals of time and may be used in future shipboard power systems. Since the inclusion of pulsed power loads in a power system may cause a much larger variation in power demand than other loads, it makes energy management a crucial task. The energy storage system, which is being discussed in this research work, consists of an energy storage device and an interface to the main power system. Energy can be stored in any of the following storage mediums

1. Battery Energy Storage
2. Flywheel Energy Storage
3. Capacitor Energy storage
4. Fuel Cell Energy Storage
5. Superconducting Magnetic Energy Storage.

Irrespective of the energy storage device, the overall energy storage system should have the capability to provide a high-energy pulse in conjunction with the main power source. To determine the requirements of an energy storage system for supporting pulsed power loads, one needs to answer the following queries:

1. What are the effects of pulsed power loads on the supply current?
2. What needs to be the rating of an energy storage interface for a given generation power?
3. What needs to be the energy storage capacity of the storage device?

1.2 Objective of this Research Work

Future naval shipboard power systems will be based on an integrated power system architecture. In this type of architecture, it is required to satisfy the energy needs of the propulsion system, which is integrated with service loads and pulsed power loads. Pulsed power loads require energy in a short time interval and their power profile is expressed using two properties: the energy drawn by a pulse and the time between each pulse. Hence energy storage systems may be used if the demands of a pulsed power load system exceed the capability of the supply. The maximum capacity of the supply could be exceeded or in the case of supplies such as gas turbine generators, the capability of the generator to increase its output has a ramp rate that could be exceeded by the pulsed power load system. The challenge is to determine the requirements of the energy storage interface that can provide the needed load leveling. It is assumed that the energy storage interface is a three-phase power electronic converter. The energy storage device is connected to the main power system on the AC side through a three-phase power

electronic converter. This research work investigates a method for determining the ratings of the three-phase power electronic converter and the required energy storage capacity based on the parameters of the pulsed power load and the system.

1.3 Thesis Overview

For the analysis of energy storage systems to compensate pulsed power loads in a distribution system, an analytical tool is developed that allows the user to specify the time interval between each pulse, the energy requirement of a pulse and the power system parameters. The outputs of the analytical tool are the current rating of the energy storage interface and the energy storage capacity required. The supply currents of pulsed power load systems are not periodic due to the time variance of pulsed power load parameters. Therefore, such loads cannot be described in terms of active, reactive and apparent powers making analyses of supply currents and determination of system ratings more difficult. The method used in this thesis for determining the ratings of an energy storage system utilizes an orthogonal decomposition of pulsed power load supply currents computed within a sliding window. The developed tool can be used to obtain information on energy storage systems for a wide range of pulsed power load profiles.

In order to validate the results obtained from the analytical tool, a simulation of a power system with a pulsed power load model was developed in Matlab/Simulink. The pulsed power load parameters are initialized by the simulation based on minimum loss criteria using time interval between each pulse, the energy requirement of a pulse and the power system parameters as inputs. The moving window discrete Fourier transform is used to determine the complex RMS value of the fundamental harmonic of the load

current. Then, the load current is decomposed into active, reactive and harmonic components. The signals obtained from the decomposition are also useful in generating the control reference signals for energy storage interface. These components act as reference signals to the active, reactive and harmonic compensators, which inject their corresponding currents into the grid. For active power compensation the compensator takes into account the given generation and calculates the additional active power required to satisfy the pulsed power load demand and the active current corresponding to this active power is injected into the grid. Hence the energy storage device and its interface to the main power system act as the energy storage system, which responds to the sudden change in active power if the load demand exceeds generation. The results obtained from the simulation are then compared with the results obtained from the analytical tool.

1.4 Thesis Organization

The contents of this thesis are summarized as follows. Chapter II discusses the basic concept of the All Electric Ship. It gives a detailed overview of Integrated Power System architectures, which are being considered for implementation in the future shipboard power systems. It gives examples of the pulsed power loads in future electric ship power systems and also illustrates the problem of energy management.

Chapter III provides background information about the signal processing techniques, which can be used in power electronic applications for periodic and aperiodic signals. The moving window discrete Fourier transform is discussed in detail. It elucidates the properties of pulsed power load system currents and its decomposition

using an appropriate orthogonal decomposition based on the Current's Physical Components Power Theory.

Chapter IV discusses the modeling of a pulsed power load system in MATLAB/Simulink and gives an overview of pulsed power load system compensation. The later part of the chapter contains the analytical approach to determine the ratings of the energy storage interface in the power system with pulsed power load using the pulsed power load profile, pulsed power load charging system parameters, and available generator active power as input parameters.

Chapter V deals with the application of the proposed analytical tool and its validation by comparing with data obtained from simulation tool, and then the analytical tool is applied to get the information on energy storage systems for a wide range of pulsed power load profiles.

Chapter VI presents conclusions and suggestions for future work based on the proposed analysis.

CHAPTER II

DESCRIPTION OF THE ALL-ELECTRIC SHIP

2.1 Concept of the All Electric Ship

Naval ships with electric propulsion systems allocate substantial amounts of power exclusively for the propulsion system. The electric propulsion system consists of three important components:

1. Generator driven by a prime mover
2. Motor drive system
3. Propulsion motor coupled with the ship propeller through a shaft.

The prime mover acts as a mechanical input to the AC generator, which converts mechanical energy into electrical energy. The motor drive system and the propulsion motor have bi-directional control interface. The developing technologies in electrical machines, power electronics and controls have made this kind of configuration more beneficial over the previous decade. Figure 2.1 shows the electric ship propulsion system [1].

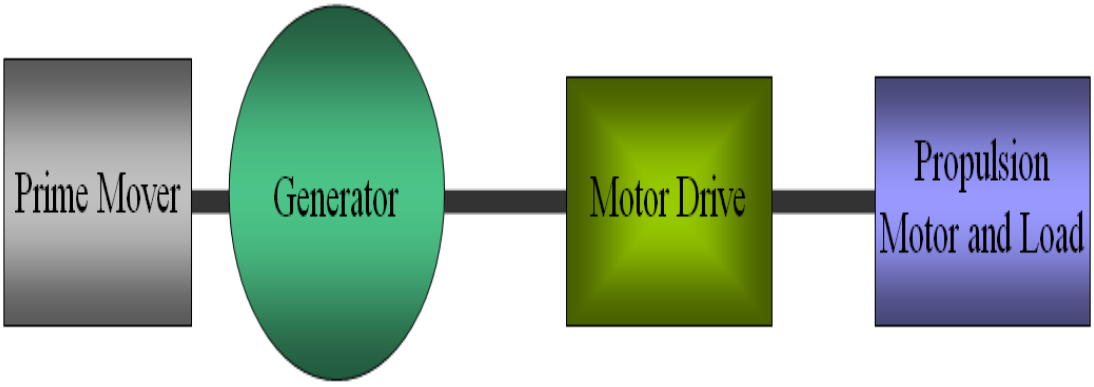

Figure 2.1 Electric Propulsion System

The primary motive of the All Electric Ship Concept is to unlock the power consumed by the electric propulsion system so that it may be distributed to a ship's high power electrical loads. The idea is to integrate the electric power generation and distribution with the electric propulsion system as shown in Figure 2.2. Hence this concept is called the Integrated Electric Power System (IPS). The technological enhancements in solid-state semiconductor devices, electrical machines and energy storage devices have enabled many improvements in IPS architecture which in turn will improve the following characteristics of the future naval warships [1]:

1. Power density
2. Efficiency
3. Design flexibility
4. Survivability
5. Economy

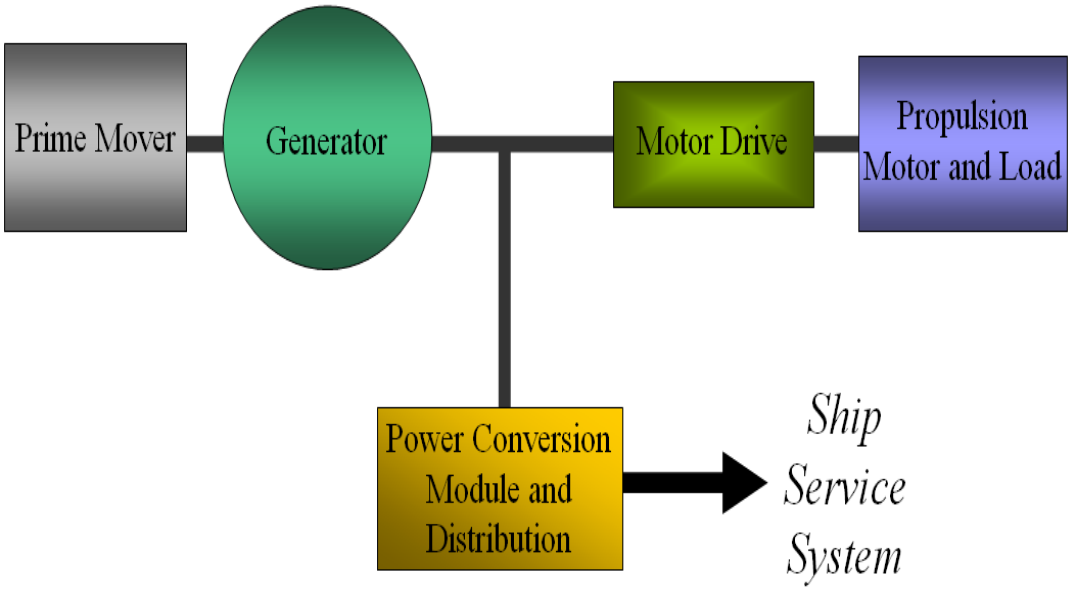

Figure 2.2 Integrated Propulsion System

2.2 IPS Architecture in Future Ship Board Power Systems

The IPS architecture has gone through much advancement since its initiation. The following sections will describe three major test cases, which were proposed by the Electric Ship Research and Development Consortium.

2.2.1 US Navy Integrated Power System Test Facility

The IPS test system for US Navy shown in Figure 2.3 was built and first tested in 1999. It consists of a 21 MW, 4160 V gas turbine generator set connected to a 4160 V, 60 Hz bus. A harmonic filter and pulse-width modulated (PWM) motor drive is connected to the 4160 V bus. The PWM motor drive consists of a PWM AC converter with three channels, which has five phases per channel and a fifteen phase, 150 RPM induction motor [2]. The actual set up of the US Navy integrated power system test facility is shown in Figure 2.4.

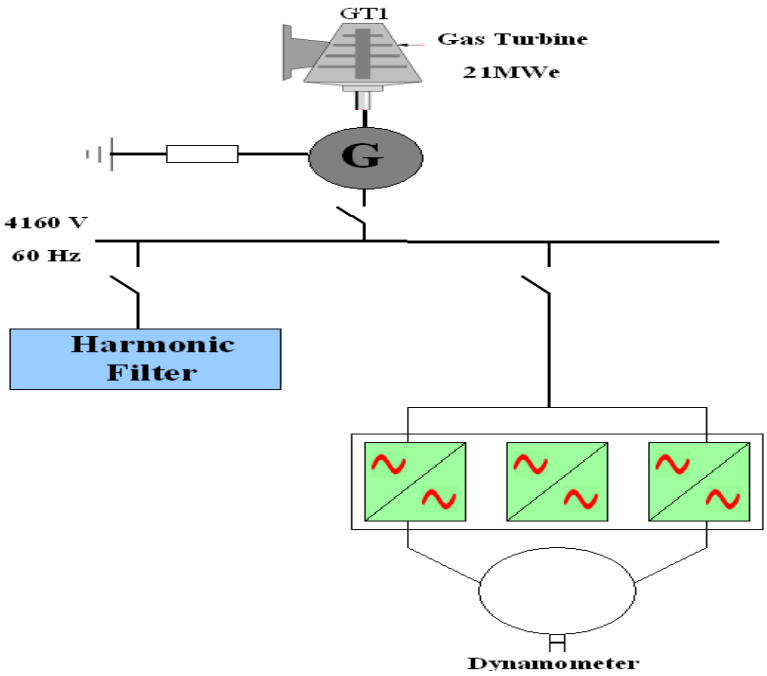

Figure 2.3 US Navy Integrated Power System.

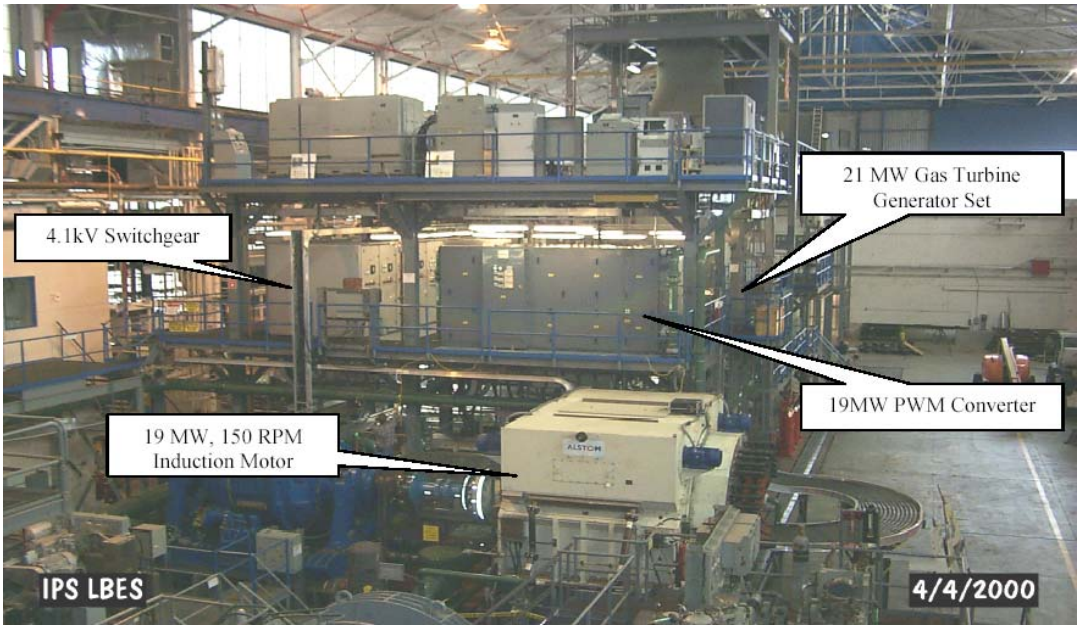

Figure 2.4 Actual Set Up of the US Navy Integrated Power System Test Facility [3]

This test facility was mainly used to study the characteristics of a PWM drive, which is considered as the paramount part of the IPS [3].

2.2.2 ONR Reference System

The ONR reference system shown in Figure 2.5, which has been installed at Purdue University, is a reduced scale IPS. It consists of the AC Generation and Propulsion Testbed and DC Zonal Ship Service Distribution Testbed [4]. The ONR has set its sight on a future surface combatant with an IPS of 100 MW of generation power [4]. The reference system configuration gives a clear idea of the IPS in a naval combatant ship and the future systems will be based on this configuration.

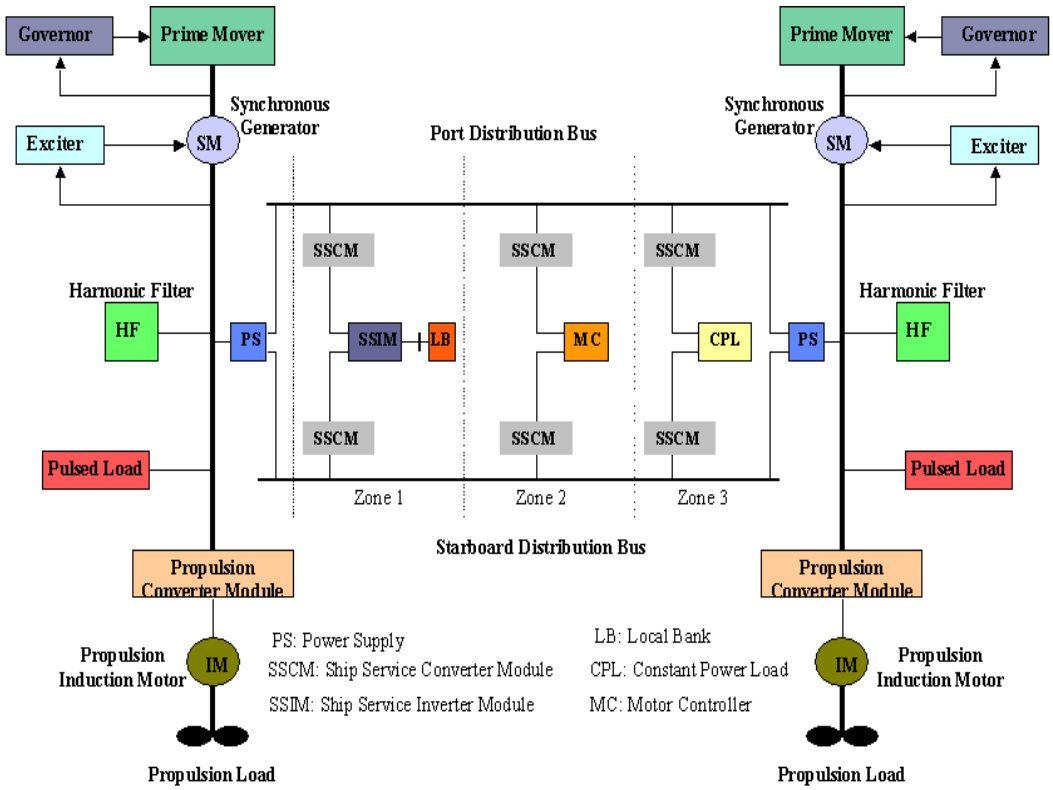

Figure 2.5 ONR Reference System Configuration.

- *AC Generation and Propulsion Testbed*

It consists of two AC propulsion buses which are supplied by a 150Hp four-quadrant dynamometer system as prime mover and governor, a synchronous machine rated at 59 kW with an output voltage of 520-590 V_{l-lRMS}, a wye-connected LC harmonic filter, a pulsed load and AC induction motor drive rated 37 kW, 1800 rpm and 460 V_{l-lRMS} connected to a load emulator [4].

- *DC Zonal Ship Service Distribution Testbed*

It consists of two 15 kW ship service power supplies with 480 V 3-phase AC diode rectifier bridge feeding a buck converter to yield 500 V DC, six 5 kW ship service converter modules to convert 500 V DC distribution power to 400 V DC, 5 kW ship service inverter modules to convert 400 V DC to 3-phase 230 V AC power, a 5 kW 3-phase inverter as a motor controller and a 5 kW buck converter as a constant power load [4].

2.2.3 Notional DD (X) Power System Model for Future Electric Ship

The Center of Electromechanics at University of Texas is currently involved in development of a ship power system model that depicts the IPS architecture in future electric ships. The future DD (X) power system model has been built using MATLAB/Simulink platform. The parameters of the model were based on the data provided by Syntek to Electric Ship Research and Development Consortium members [5]. The model has some considerable changes when compared to the ONR reference system as it can be observed in Figure 2.6.

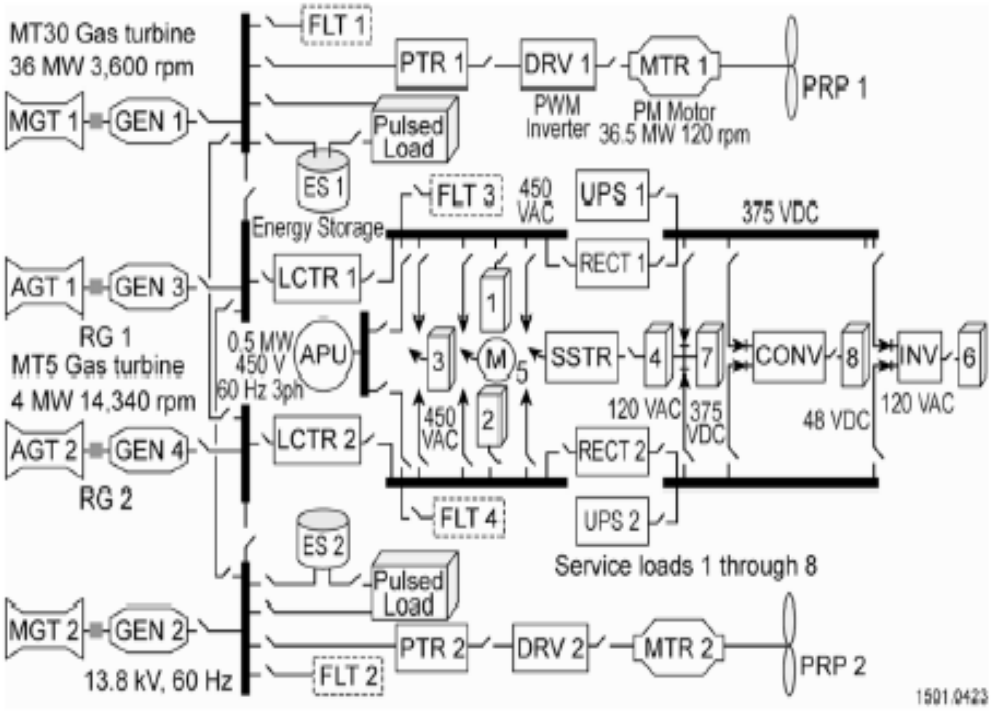

Figure 2.6 Notional DD (X) Power System for Future Electric Ship [5].

The model consists of two main gas turbine-generator sets of 36 MW each and two auxiliary gas turbine-generator of 4 MW each, supplying a total active power of 80 MW. The propulsion train consists of 13.8 kV/4.16 kV three-phase transformer connected to an uncontrolled rectifier which in turn is connected to a pulse width modulated inverter, which drive the propulsion motor. The ship service distribution system consists of two load-center transformers, two rectifiers, a ship service transformer, an inverter, a DC-DC converter and eight different ship service loads [5].

In this research work, some of the parameters of the Notional DD (X) Power System are used to represent the power system model due to the fact that this system incorporates many of the attributes that are expected in a future shipboard power system.

Thus, the generator active power capacity (80 MW) and the generation voltage (13.8 kV) are considered as the system parameters for the three-phase power supply.

2.3 Pulsed Power Loads in Shipboard Power Systems

Pulsed power loads are described as loads that require a substantial amount of energy in a very short period of time in the form of pulses. Data of a pulsed power load as in Reference [6] is given as follows:

- Pulse duration is 6 to 9 milliseconds with an output pulse power of 10 GW.
- Typical voltage is 10 kV at a load current of 10^6 A.
- Input energy per pulse of 160 MJ.
- Operating rate is 6 pulses per minute, which lasts for operating time of 3 minutes.
- Average power is 13.3 MW taken over 1 minute.

Since the pulsed power loads require energy on the order of hundreds of MJ, they are not directly connected to the generator in order to avoid the application of a large pulse to the overall power system. The pulsed power load is connected to the main generator bus through an energy storage system in the notional DD (X) power system in Figure 2.6. In general pulsed power loads are connected to the distribution system through a charging system, used to charge an Intermediate Energy Storage Module (IESM). The pulsed power load is connected to the IESM in parallel. All of these components form a pulsed power load system. The structure of the Pulsed Power Load System is shown in Figure 2.7.

In this research work a three-phase diode bridge rectifier is considered as the charging system and a capacitor is considered as the IESM. The pulsed power load system which consists of a pulsed power load connected to an IESM (capacitor) with a charging system (three-phase diode bridge rectifier and an inductor), is shown is Figure 2.8. It is important to differentiate between the IESM and the energy storage systems that aid the main generator. The IESM is an integral part of the pulsed power load system, while the energy storage system aids the generators in supplying the pulsed power load system. The energy storage system is connected to the AC side of the power system, it consists of an energy storage device and an interface to the main power system as discussed in Section 1.2 of Chapter 1.

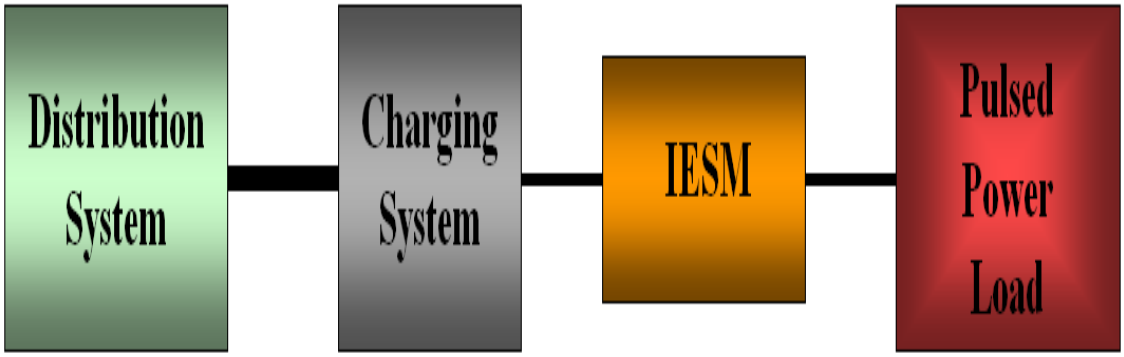

Figure 2.7 Pulsed Power Load System

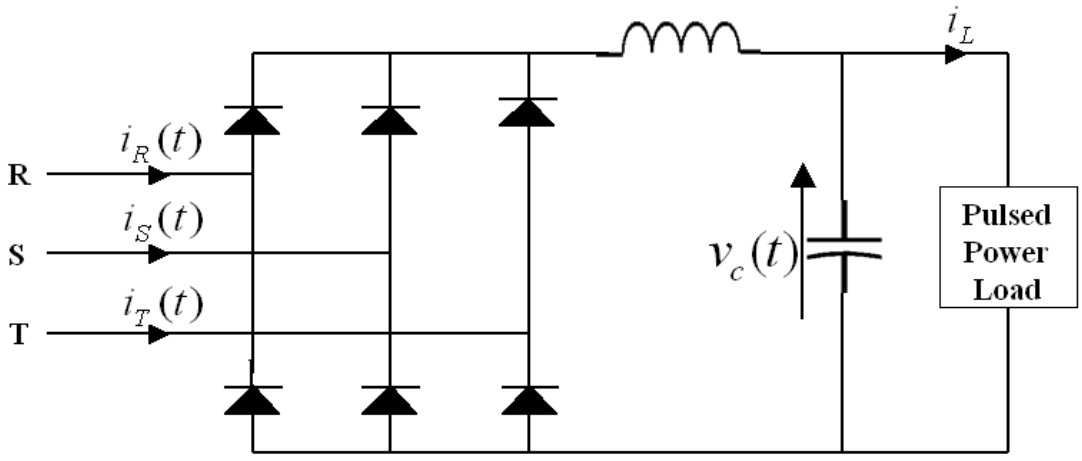

Figure 2.8 Pulsed Power Load Connected to the AC Side through a Diode Bridge Rectifier, Inductor and a Capacitor.

The pulsed power load takes in energy from the distribution system through a six-pulse diode rectifier for a few seconds while the capacitor charges. The charge is amassed in the capacitor and the charging time depends on the inductor and resistance of the charging system. When a pulse occurs, the capacitor discharges releasing the stored energy within a time that is equal to the width of the pulse and produces a large discharging current on the order of a few hundred kA. The harmonics in the supply current are due to the six-pulse diode bridge rectifier and its magnitude depends on input current of the pulsed power load. An example waveform of input current, i_L is shown in Figure 2.9. The waveform of input current i_L, supply current in phase R, $i_R(t)$ is shown in Figure 2.10 and the capacitor voltage $v_c(t)$ is shown in the Figure 2.11. Figure 2.12 shows the supply current and load current waveform for a time scale (x-axis) of 1 second after the pulse occurs. It can be observed from Figure 2.12 that a pulse causes a considerable amount of variation and harmonic distortion in the supply current.

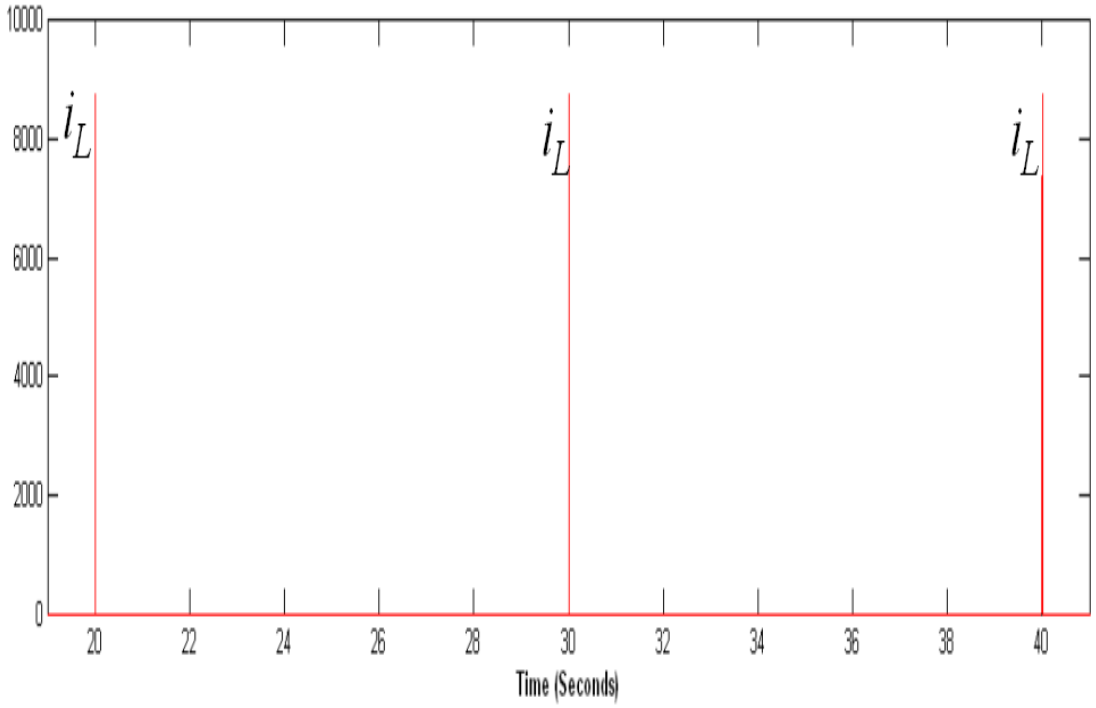

Figure 2.9 Pulsed Power Load Input Current

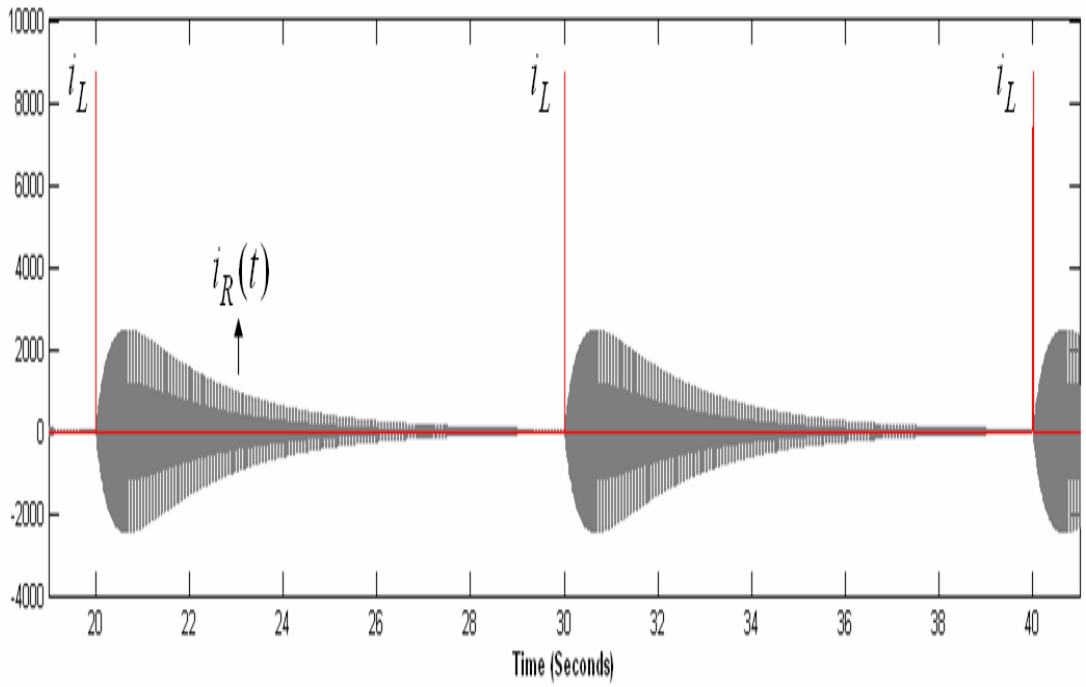

Figure 2.10 Pulsed Power Load System Supply Current and Input Current.

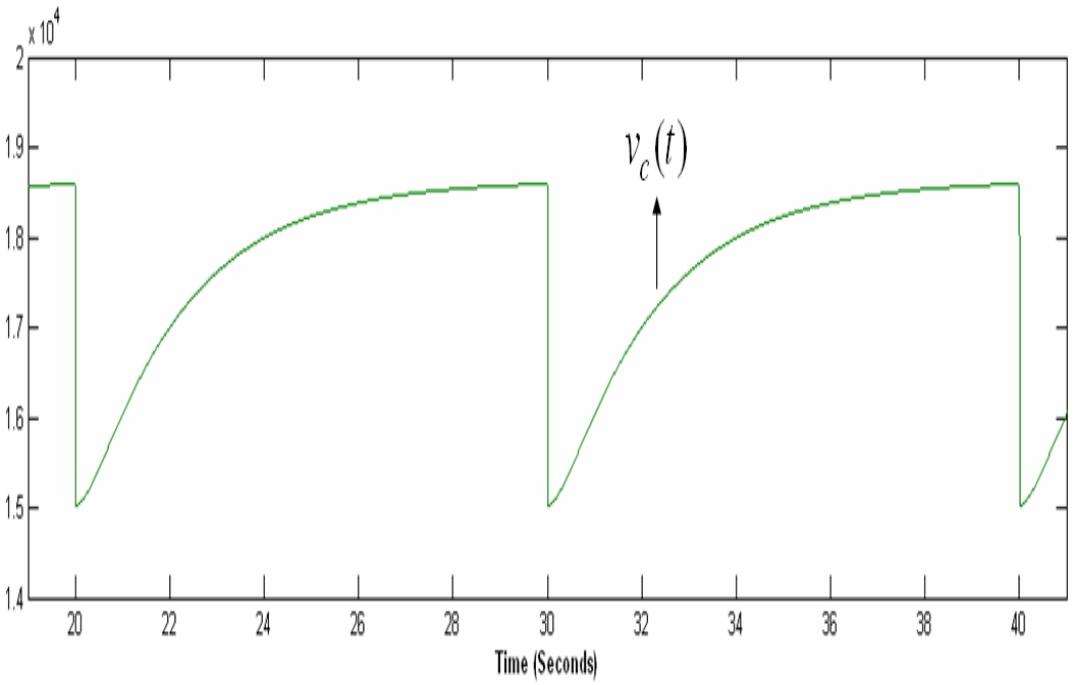

Figure 2.11 Capacitor Voltage

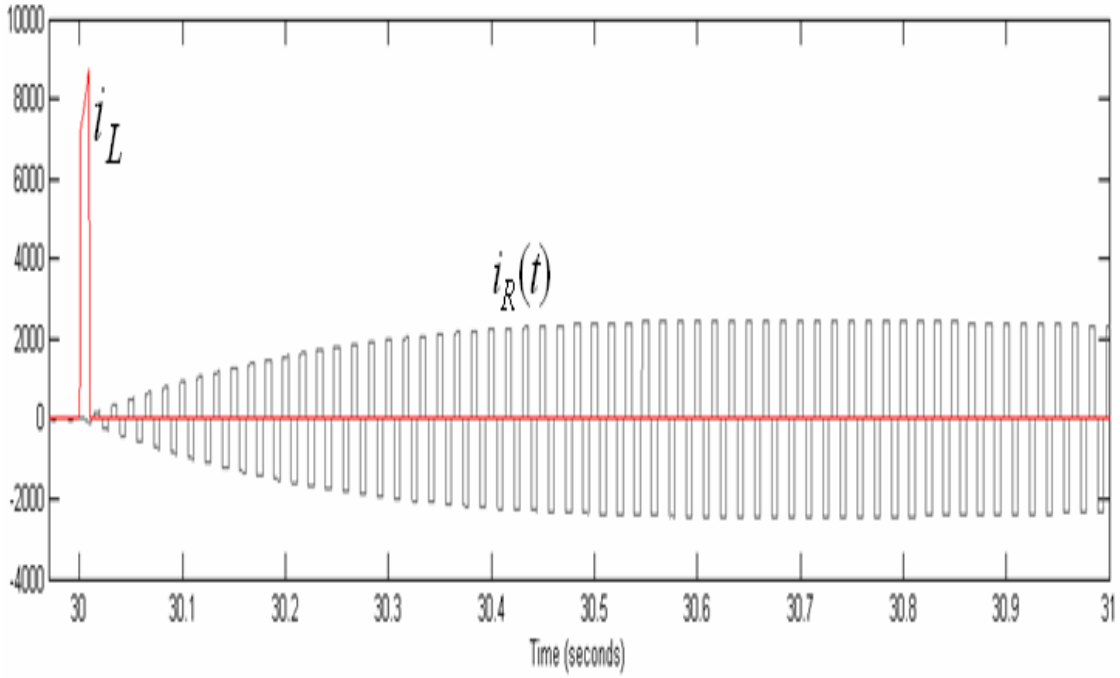

Figure 2.12 Supply Current and Input Current of a Pulsed Power Load

2.4 Energy Management for Shipboard Power Systems

Energy management is considered as a critical aspect of the future electric ship concept because the generation power will not be sufficient if all the loads are operating at the same time. Hence there are priorities for the operation of loads and energy storage devices to support the energy management process. An Electric Ship may consist of four types of loads: critical loads or pulsed power loads, which require a high magnitude of energy during their operating conditions; non-critical loads or non-vital loads that can be operated as desired, i.e. ship service loads; semi-vital loads that are operated most of the time but with energy requirements that are dependent on the speed of the ship, such as propulsion loads; and vital loads, which are operated all the time. The critical loads when operated in combination with any one of the mentioned loads may result in an overload of the generators. Hence an energy buffer system is needed. Energy storage devices are such buffers that are used to compensate the sudden load demand due to critical loads.

There are many eligible sources of stored energy in an electric ship; these include the electric ship's kinetic energy, the energy obtained due to the rotational motion of the propulsion drive and other alternative energy storage systems [6]. The alternative energy storage devices are of several kinds, they are

- Flywheel energy storage system.
- Fuel cell energy storage system.
- Superconducting magnetic energy storage system.
- Battery base energy storage system.

- Capacitor based energy storage system.

The flywheel energy storage system is preferred for use with the rail gun weapons and is available now in a wide range of designs to meet the future electric ship requirements [6]. In the widely used configuration of the flywheel energy storage system, an indirect field oriented controlled induction machine drive is integrated with back-to-back voltage source converters coupled through a DC link. This configuration allows bi-directional power flow so that the flywheel's kinetic energy can be charged and discharged accommodating load variation. Figure 2.12 shows a future combatant electric ship power system, which consists of five flywheel energy storage systems S1 to S5, where S1 is used to compensate power supply transients and S2 to S5 are used to compensate for critical loads [6].

Some of the examples of pulsed Power Loads are high power rail gun, high power laser weapons, high power microwave weapons and active armour that is designed to dynamically prevent damage to a ship [6]. Hence different energy storage systems may be used for different types of pulsed power load systems based on their energy profile. Therefore there may be any energy storage systems at S1 to S5 in Figure 2.12 in future electric ships. This research work is not restricted to any particular type of energy storage system and pulsed power load system. It determines the AC side effects on load current due to any pulsed power load system using Recursive Discrete Fourier Transform in conjunction with an orthogonal decomposition based on the Current's Physical Components Power Theory. This information is then used to determine the ratings of the energy storage interface and the energy storage capacity for any energy storage system

S4 and S5 in a power system with a pulsed power load system L1 (EMCAT – Electromagnetic Catapult) as shown in Figure 2.8. The analysis method is also suitable for the generation of control signals for the energy storage system.

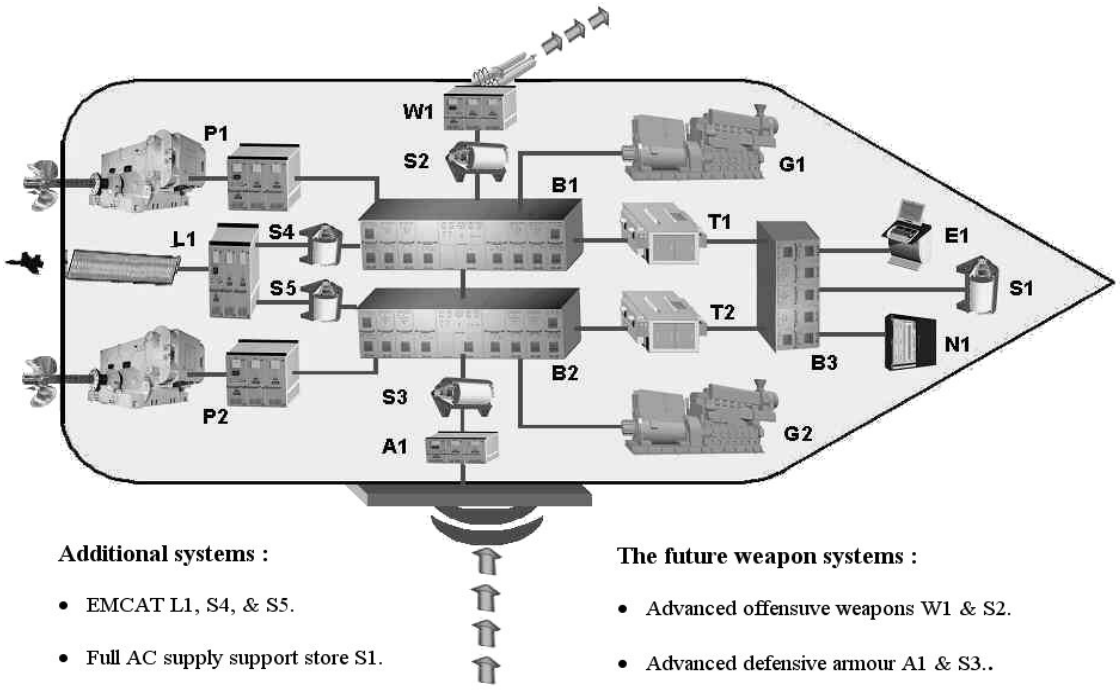

Figure 2.13 A Future Combatant Electric Ship [6].

CHAPTER III

ANALYSIS OF APERIODIC CURRENTS IN SHIPBOARD POWER SYSTEM

3.1 Signal Processing in Power Electronic Applications

A generator supply current may contain several frequency components. Hence frequency analysis has to be performed on the current signal to separate any harmonic components from the fundamental component. Two of the popularly used methods for frequency analysis in power electronics are the Fourier series and Fourier transform. Generally for power electronic applications, Fourier series is used for frequency analysis of periodic signals and Fourier transform is used for frequency analysis of aperiodic signals. The following sections will discuss the Fourier series and Fourier transform, for signals with a particular kind of periodicity.

3.1.1 Fourier Series

The basics of Fourier series that are suited for power electronic applications are discussed in reference [7]. The Fourier series is a tool for mathematical representation of a periodic signal. It enables the decomposition of the periodic signal as a sum of harmonic sinusoids. A periodic signal with a fundamental period $T = \frac{1}{f_1}$, where f_1 is the fundamental frequency can be represented as shown in equation.

$$x(t) = \sum_{n=-\infty}^{n=\infty} s_n e^{jn\omega_1 t} \tag{3.1}$$

$\omega_1 = 2\pi f_1$ radians/sec

$n = 0,\pm1,\pm2,\pm3,.....$

s_n - Co-efficient which determines the shape of the waveform of frequency nf_1.

The signal $x(t)$ can be represented in Fourier series if it satisfies the Drichlet conditions. The conditions are:

- $x(t)$ should contain finite number of maxima and minima during any period.
- $x(t)$ should have a finite number of discontinuities in any period.
- $x(t)$ should be absolutely integrable in any period.

If we neglect the discontinuity factor, the Fourier series can be represented in the form as shown in Equation 3.2.

$$x(t) = a_0 + \sum_{n=1}^{n=\infty} a_n \cos n\omega_1 t + \sum_{n=1}^{n=\infty} b_n \sin n\omega_1 t \tag{3.2}$$

$$a_0 = \frac{1}{T}\int_0^T x(t)dt \tag{3.3}$$

$$a_n = \frac{2}{T}\int_0^T x(t)\cos(n\omega_1 t)dt \tag{3.4}$$

$$b_n = \frac{2}{T}\int_0^T x(t)\sin(n\omega_1 t)dt \tag{3.5}$$

The expression in Equation 3.2 is not appropriate for use in linear circuit analysis. Therefore the classical Fourier series has to be expressed in complex form as given in Equation 3.6

$$x(t) = X_0 + \sqrt{2}X_n \,\mathrm{Re}\sum_{n=1}^{n=\infty} X_n(\cos(n\omega_1 t) + j\sin(n\omega_1 t)) \tag{3.6}$$

$$X_0 = a_0 \tag{3.7}$$

$$X_n = \frac{a_n - jb_n}{\sqrt{2}} \tag{3.8}$$

substituting Equation 3.4 and Equation 3.5 in Equation 3.8 we get

$$X_n = \frac{\sqrt{2}}{T}\int_0^T x(t)(\cos(n\omega_1 t) - j\sin(n\omega_1 t))dt \tag{3.9}$$

$$X_n = \frac{\sqrt{2}}{T}\int_0^T x(t)e^{-jn\omega_1 t}dt \tag{3.10}$$

X_n - Complex RMS value of the n-th order harmonic.

3.1.2 Properties of Pulsed Power Load System Supply Currents

The supply current of a pulsed power load system does not obey the periodicity property because a pulsed power load system supply current, say $i(t)$ does not hold true for the periodicity equation shown in Equation 3.11

$$i(t) = i(t \pm nT) \tag{3.11}$$

Where n is any integer and T, called a period is a non-zero real number.

These currents are called semi-periodic currents i.e. they obey the properties of the subset of non-periodic current. The semi-periodic currents are signals that lost periodicity due to the time variance of load parameters and hence cannot be expressed in terms of Fourier series. The only positive aspect of pulsed power load system supply currents for decomposition purpose is that the permanent energy transfer with such currents is associated only with their semi-sinusoidal fundamental component that is in

phase with the supply voltage and hence the period T of the supply voltage is considered as the time frame for analysis of power properties of the power systems with pulsed power loads [8].

3.1.3 Moving Window Discrete Fourier Transform

If a periodic signal is perturbed such that it is aperiodic over some interval, it may not be appropriate to update the adjusted frequency components after the completion of each cycle. In such a case a moving window discrete Fourier transform may be used [9]. The algorithm uses a simple moving window approach, which consists of a First in, First out data array that accepts N data values. Initially the buffer must have a zero value. A circular index-pointer selects the current data value, if a new data value is entered to the buffer-array then the old value is overwritten and the index is incremented modulo N, in this way a new window is obtained. This moving window approach illustrates that the Fourier coefficients can be calculated at any new window by only considering the difference between the new value and the old value multiplied with the respective sine or cosine functions based on the whether it is a real or imaginary value [10]. As can be seen in Figure 3.1, the observation window of size N (number of samples within the window) keeps moving by including a new sample and excluding the old sample. The Fourier coefficients are computed for the samples within the window.

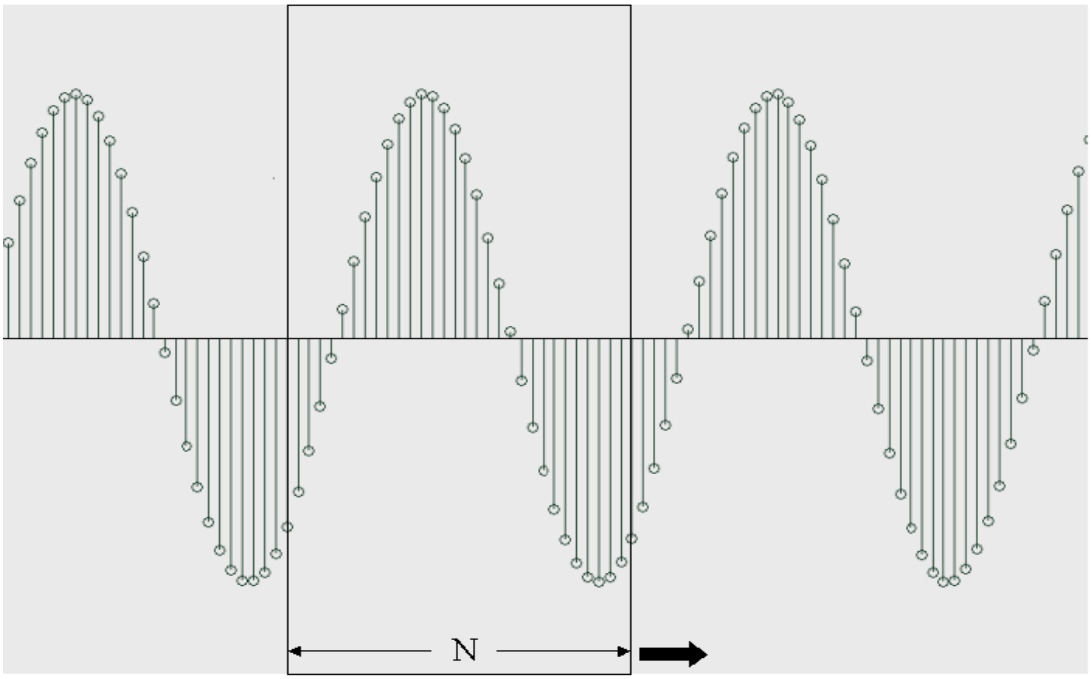

Figure 3.1 Illustration of Moving Window DFT

For non-periodic signals that have a different period other than T (period of the supply voltage), the complex RMS value X_1 that is calculated from N samples of $x(k)$ taken over the window of the period T, which is given by

$$X_1 = \frac{\sqrt{2}}{N}\sum_{k=0}^{N-1} x(k)e^{-j\left(\frac{2\pi}{N}\right)k} \tag{3.12}$$

The Equation in 3.12 will vary with the moving window. When the new sample $x(k)$ is obtained by the buffer array, then the complex RMS value referred to as running complex RMS value of the fundamental harmonic and denoted by $\tilde{\approx}X_1(k)$ can be calculated using Equation 3.13 [11]. The symbol "≈" implies that the value keeps varying with time as the window moves forward.

$$\tilde{\tilde{X}}_1(k) = \tilde{\tilde{X}}_1(k-1) + \left[(x(k) - x(k-N))\right] e^{-j\left(\frac{2\pi}{N}\right)} \tag{3.13}$$

For current decomposition, which will be discussed in the following sections, the Moving Window DFT is used to detect the complex RMS value of the fundamental harmonic of the load current in a power system with a pulsed power load. The application of Moving Window DFT in this research will be discussed in Section 3.3 of Chapter 3.

3.2 Current Physical Components' Power Theory

Czarnecki proposed the Current's Physical Components (CPC) Power Theory [12], which was developed in the frequency domain and can be used for all single-phase and three-phase non-linear systems. This theory provides an orthogonal decomposition of the currents and voltages in a system. The current components are decomposed based on their respective physical phenomena. Let us confine our discussion in this section to a three-phase, three-wire system with linear, time-invariant load supplied from a sinusoidal symmetrical voltage source of positive sequence as shown in Figure 3.2.

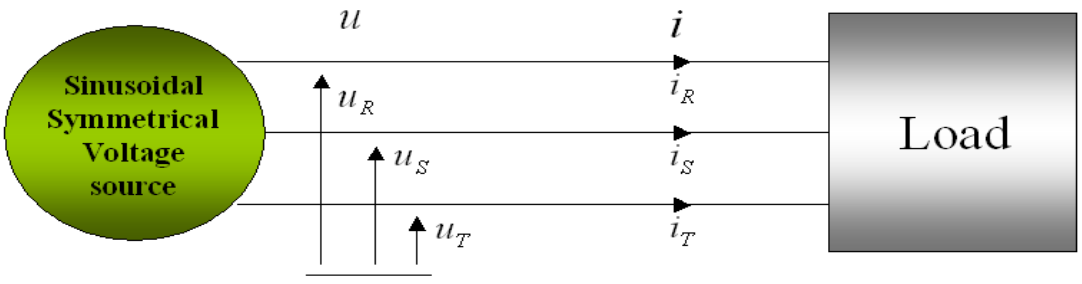

Figure 3.2 Three-Phase System with Linear, Time-Invariant Load

For the load shown in Figure 3.2 there is a balanced and resistive load as shown in Figure 3.3 with the same voltage and an equivalent active power P that is given by Equation 3.14

$$P = G_e \|u_R\|^2 + G_e \|u_S\|^2 + G_e \|u_T\|^2 = G_e \|u\|^2 = G_e V_{LN}{}^2 \tag{3.14}$$

$$i_a = \begin{bmatrix} i_{aR} \\ i_{aS} \\ i_{aT} \end{bmatrix} = G_e u \tag{3.15}$$

$$\|i_a\| = G_e \|u\| \tag{3.16}$$

G_e - Equivalent Conductance of the Load.

V_{LN} - RMS value of the line-to-neutral voltage.

i_a -Active Current of the Balanced and Resistive Load

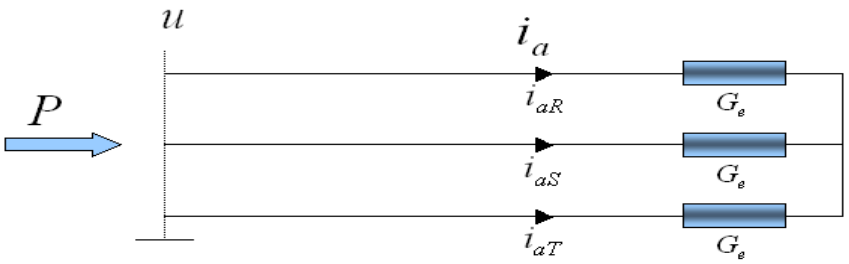

Figure 3.3 Equivalent Load with respect to Active Power

There also exists a balanced and an equivalent reactive load as shown in Figure 3.4 with the same voltage and a reactive power Q that is given by the Equation 3.17

$$Q = -B_e \|u_R\|^2 - B_e \|u_S\|^2 - B_e \|u_T\|^2 = -B_e \|u\|^2 = -B_e V_{LN}{}^2 \tag{3.17}$$

$$i_r = \begin{bmatrix} i_{rR} \\ i_{rS} \\ i_{rT} \end{bmatrix} = B_e \frac{d}{d\omega_1 t}(u) \tag{3.18}$$

$$\|i_r\| = B_e \|u\| \tag{3.19}$$

B_e - Equivalent Susceptance of the Load.

i_r -Reactive Current of the Balanced and Reactive Load.

ω_1 -Angular Fundamental Frequency in radians/second.

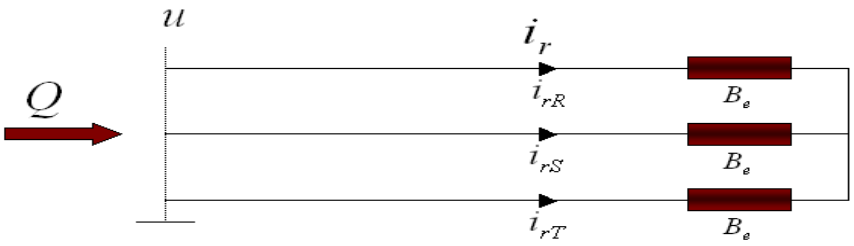

Figure 3.4 Equivalent Load with respect to Reactive Power

For any three-phase three-wire system there exists an equivalent system with a delta-connected load as shown in Figure 3.5.

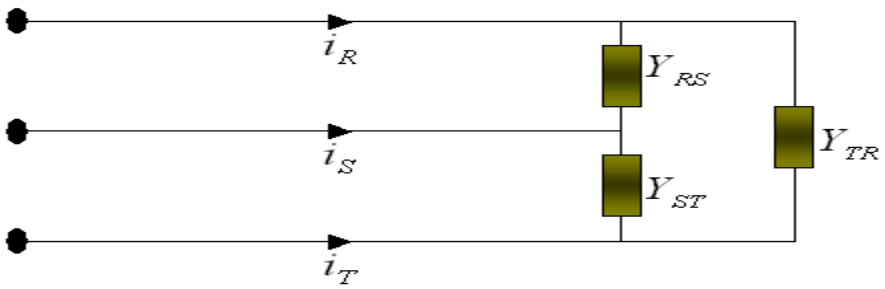

Figure 3.5 Equivalent Delta-Connected Load

The sum of three delta-connected admittances gives the equivalent load admittance Y_e as in Equation 3.20

$$Y_{RS} + Y_{ST} + Y_{TR} = Y_e = G_e + jB_e \tag{3.20}$$

If the load is unbalanced there exists an unbalanced component A that gives rise to negative sequence currents in the circuit.

$$A = -(Y_{ST} + \alpha Y_{TR} + \alpha^* Y_{RS}) \tag{3.21}$$

where, $\alpha = 1e^{\frac{j2\pi}{3}}$ and $\alpha^* = 1e^{\frac{-j2\pi}{3}}$

$$i_u = i - (i_a + i_r) = \begin{bmatrix} i_{uR} \\ i_{uS} \\ i_{uT} \end{bmatrix} \tag{3.22}$$

$$\|i_u\| = A\|u\| \tag{3.23}$$

Since this research work deals with balanced system, the concept of unbalanced admittance is not explained in detail here. Detailed explanation can be found in Reference [12]. For a balanced system, $Y = Y_{ST} = Y_{TR} = Y_{RS}$ then $A = -(1 + \alpha + \alpha^*)Y = 0$.

A - Unbalanced Admittance of the Load.

i_u -Unbalanced Current Absorbed by the Unbalanced Load.

3.3 Load Current Decomposition for a Power System with Pulsed Power Load

The power system with pulsed power load considered in this research is balanced and resistive and is supplied by a sinusoidal voltage source. For this system the supply current can be decomposed into three different components i.e. active current component of fundamental harmonic, reactive current component of the fundamental harmonic and

distorted component as shown in Equation 3.24. Figure 3.6 shows an example plot of active current waveform at the fundamental frequency along with the phase voltage. Figure 3.7 shows an example plot of reactive current waveform at the fundamental frequency along with the phase voltage. Figure 3.8 shows an example plot of unbalanced current waveform at the fundamental frequency along with the phase voltage. All of the frequency components above the fundamental frequency are lumped into one component called the distorted component. The CPC Power Theory that was discussed in the previous section is used to decompose the fundamental frequency components. Figure 3.9 shows an example plot of distorted current waveform along with the phase voltage.

$$i = i_{1a} + i_{1r} + i_d \tag{3.24}$$

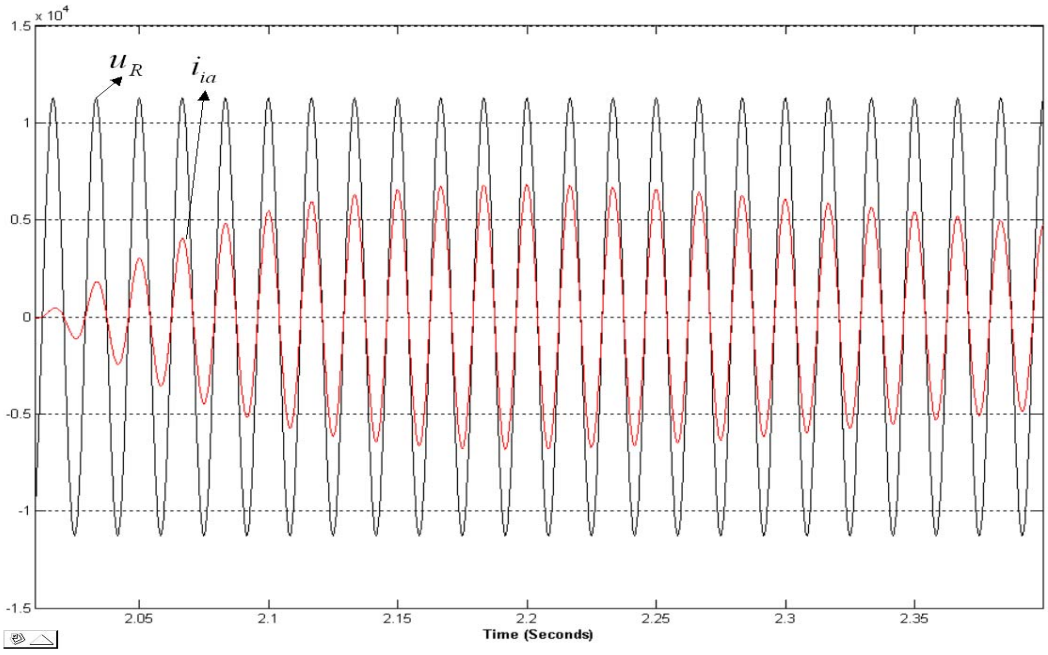

Figure 3.6 Active Current at the Fundamental Frequency with Phase Voltage

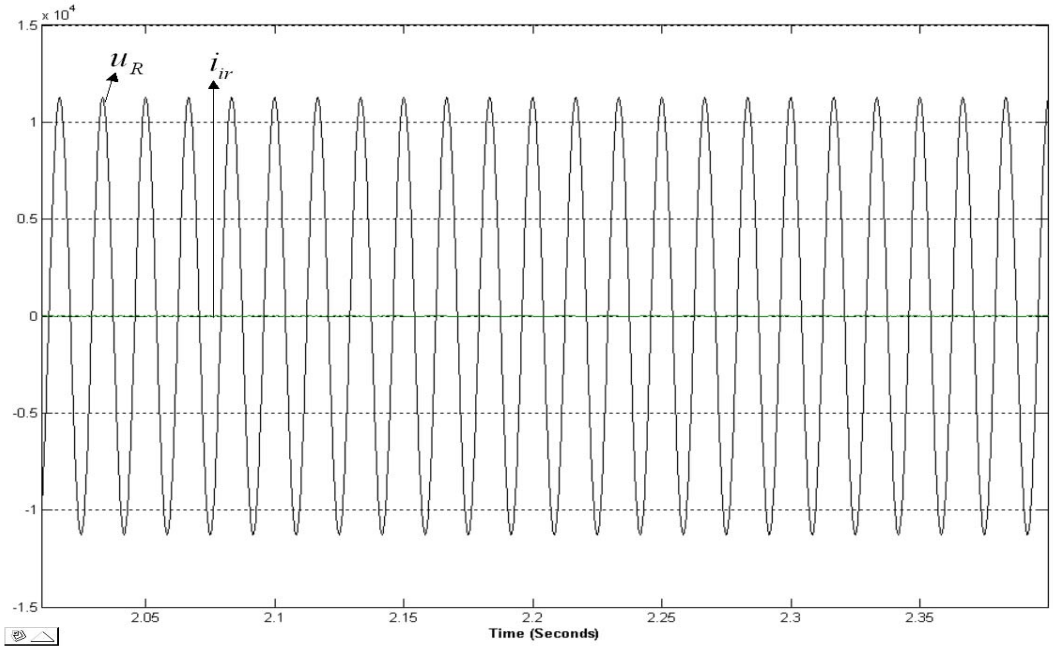

Figure 3.7 Reactive Current at the Fundamental Frequency with Phase Voltage

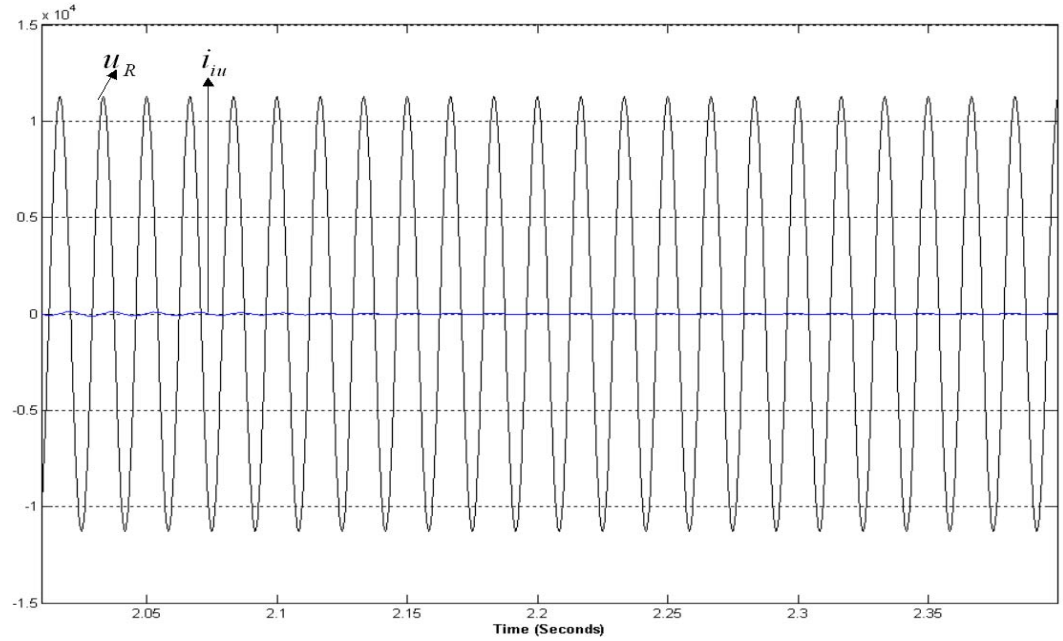

Figure 3.8 Unbalanced Current at the Fundamental Frequency with Phase Voltage

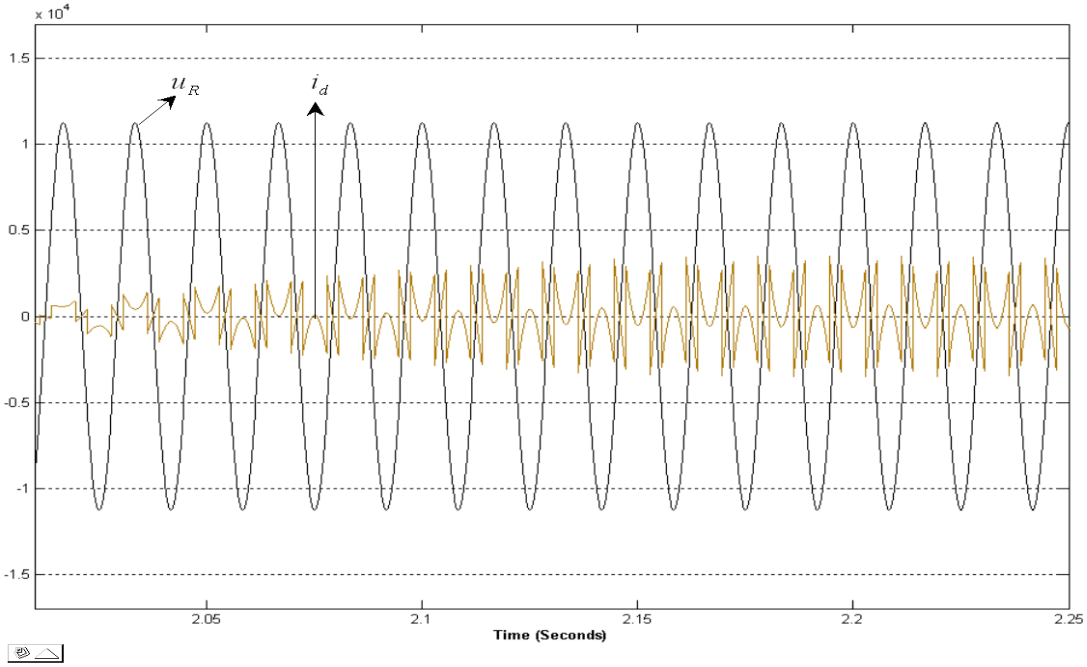

Figure 3.9 Distorted Current Waveform with Phase Voltage

These three components can be expressed as time varying quantities in terms of CPC Power theory as they vary with a change in the observation window. Hence we can conclude that these components of the supply current in a power system with pulsed power load are always time varying given the fact that the supply current is semi-periodic.

The time varying complex RMS values of the fundamental harmonic of the line currents can be given as in Equation 3.25.

$$\begin{aligned} \tilde{\tilde{I}}_R &= \tilde{\tilde{Y}}_{RS}\,\tilde{\tilde{U}}_{RS} - \tilde{\tilde{Y}}_{TR}\,\tilde{\tilde{U}}_{TR}\,, \\ \tilde{\tilde{I}}_S &= \tilde{\tilde{Y}}_{ST}\,\tilde{\tilde{U}}_{ST} - \tilde{\tilde{Y}}_{RS}\,\tilde{\tilde{U}}_{RS}\,, \\ \tilde{\tilde{I}}_T &= \tilde{\tilde{Y}}_{TR}\,\tilde{\tilde{U}}_{TR} - \tilde{\tilde{Y}}_{ST}\,\tilde{\tilde{U}}_{ST}\,, \end{aligned} \tag{3.25}$$

We know that, in a three-wire system $\tilde{\tilde{I}}_R + \tilde{\tilde{I}}_S + \tilde{\tilde{I}}_T = 0$. Hence one Equation of 3.25 is dependent on the others, which lead to an infinite number of different solutions with respect to an equivalent load admittance [13]. For this equivalent load admittance suppose if $\tilde{\tilde{Y}}_{RS} = 0$ then other two admittances are given by,

$$\tilde{\tilde{Y}}_{TR} = \frac{\tilde{\tilde{I}}_R}{\tilde{\tilde{U}}_{TR}};\ \tilde{\tilde{Y}}_{ST} = \frac{\tilde{\tilde{I}}_S}{\tilde{\tilde{U}}_{ST}} \tag{3.26}$$

The complex RMS values of the fundamental harmonic of the line currents and voltages in Equation 3.26 are obtained by applying the moving window discrete Fourier transform to the measured load side signals of currents and voltages. The equivalent admittance can be expressed as a sum of the two admittances in Equation 3.26

$$\tilde{\tilde{Y}}_e = \tilde{\tilde{Y}}_{ST} + \tilde{\tilde{Y}}_{TR} = \tilde{\tilde{G}}_{e1} + j\,\tilde{\tilde{B}}_{e1} \tag{3.27}$$

$\tilde{\tilde{G}}_{e1}$ - Equivalent conductance of fundamental harmonic of the load.

$\tilde{\tilde{B}}_{e1}$ - Equivalent susceptance of fundamental harmonic of the load.

The supply currents of the pulsed power load system are calculated from $\tilde{\tilde{G}}_{e1}$ and $\tilde{\tilde{B}}_{e1}$ values which are obtained from the Equation 3.27.

$$i_{1a} = \tilde{\tilde{G}}_{e1} \left\| \ \tilde{\tilde{u}} \ \right\| \sqrt{2} \begin{bmatrix} \cos(\omega_1 t) \\ \cos(\omega_1 t - 120) \\ \cos(\omega_1 t + 120) \end{bmatrix} \tag{3.28}$$

i_{1a} - Active current component of the fundamental harmonic of the load

$$i_{1r} = \tilde{\tilde{B}}_{e1} \left\| \; \tilde{\tilde{u}} \; \right\| \sqrt{2} \begin{bmatrix} \cos(\omega_1 t + 90) \\ \cos(\omega_1 t - 120 + 90) \\ \cos(\omega_1 t + 120 + 90) \end{bmatrix} \tag{3.29}$$

i_{1r} - Reactive current component of the fundamental harmonic of the load

$$i_1 = i_{1a} + i_{1r} \tag{3.30}$$

Since the fundamental harmonic is not a constant, but a function of time, the current i_1 is not a sinusoidal current. It is referred to as a fundamental semi-harmonic of the supply current. Also the active and reactive currents in Equation 3.28 and Equation 3.29 are not sinusoidal currents. The distorted component is obtained by subtracting the fundamental semi-harmonic from the supply current [8].

$$i_d = i - i_{1a} + i_{1r} \tag{3.31}$$

i_d - Distorted current component.

In this research work the power system considered contains the circuit with semi-periodic current. Therefore the Moving Window DFT and the CPC Power Theory can be used effectively to associate specific currents and powers with distinctively different power phenomena [8].

CHAPTER IV

DETERMINATION OF THE RATINGS OF THE ENERGY STORAGE SYSTEMS

4.1 Modeling of a Pulsed Power Load System

The pulsed power load is modeled as a current source with a known power profile, which draws current based on the voltage across the DC bus. Hence the voltage at each step is determined and the corresponding current is calculated following the power profile. The power profile of the pulsed power load model is calculated based on the input parameters. The pulsed power load's inputs are the energy profile (i.e.) energy in joules (E); time duration of the pulse; width (W); rise time (t_r) and fall time (t_f) of the pulse. Figure 4.1 shows the pulsed power load system model in MATLAB/Simulink. The power profile of a pulse is a trapezoidal waveform with a height (H) given by Equation 4.1.

$$H = \frac{2E}{(2W - t_r - t_f)} \tag{4.1}$$

The AC current is rectified through a three-phase diode bridge rectifier and there is a LC charging circuit at the DC terminals of the rectifier. The capacitor is charged through an inductor, which has some internal resistance and this charge is accumulated in the capacitor until the pulse starts. During the pulse, the energy stored in the capacitor is released in a short interval of time giving rise to a high current pulse. An example DC

current waveform at the output terminals of the diode bridge rectifier is shown in Figure 4.2.

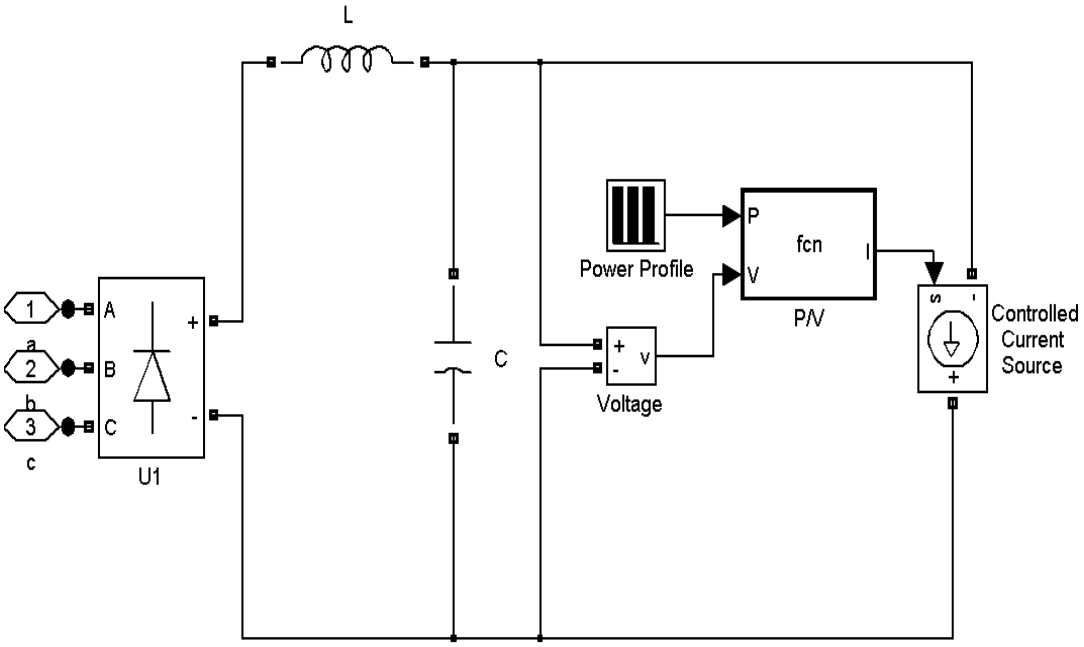

Figure 4.1 Pulsed Power Load System Model in MATLAB/Simulink

The load is programmed to replicate the properties of the pulsed power load discussed in Chapter 2, which needs three rounds of pulses. Each round consists of six pulses; the time between each pulse can be specified as the input parameter.

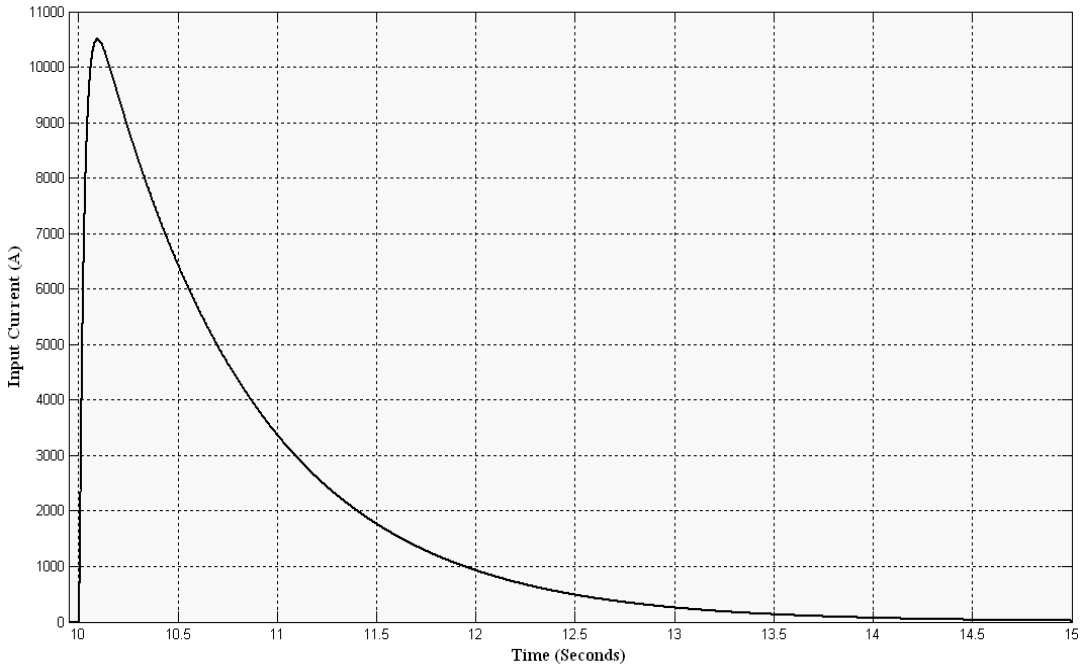

Figure 4.2 Example DC Current Waveform at the Output Terminals of the Diode Bridge Rectifier

4.2 Pulsed Power Load System Compensators

Pulsed power load system compensators have to negate the effects of variation in active and reactive power and current distortion. These two effects can be categorized by the energy storage required and the speed of variation. The active power compensation requires a substantial amount of energy storage capability but less speed of response. On the other hand the current distortion compensator requires more speed of response but does not require a considerable amount of energy storage. Hence instead of a single compensator for pulsed power load systems, it would be effective to have two separate compensators for active and reactive power variation and for harmonic distortion respectively as shown in Figure 4.3 [8].

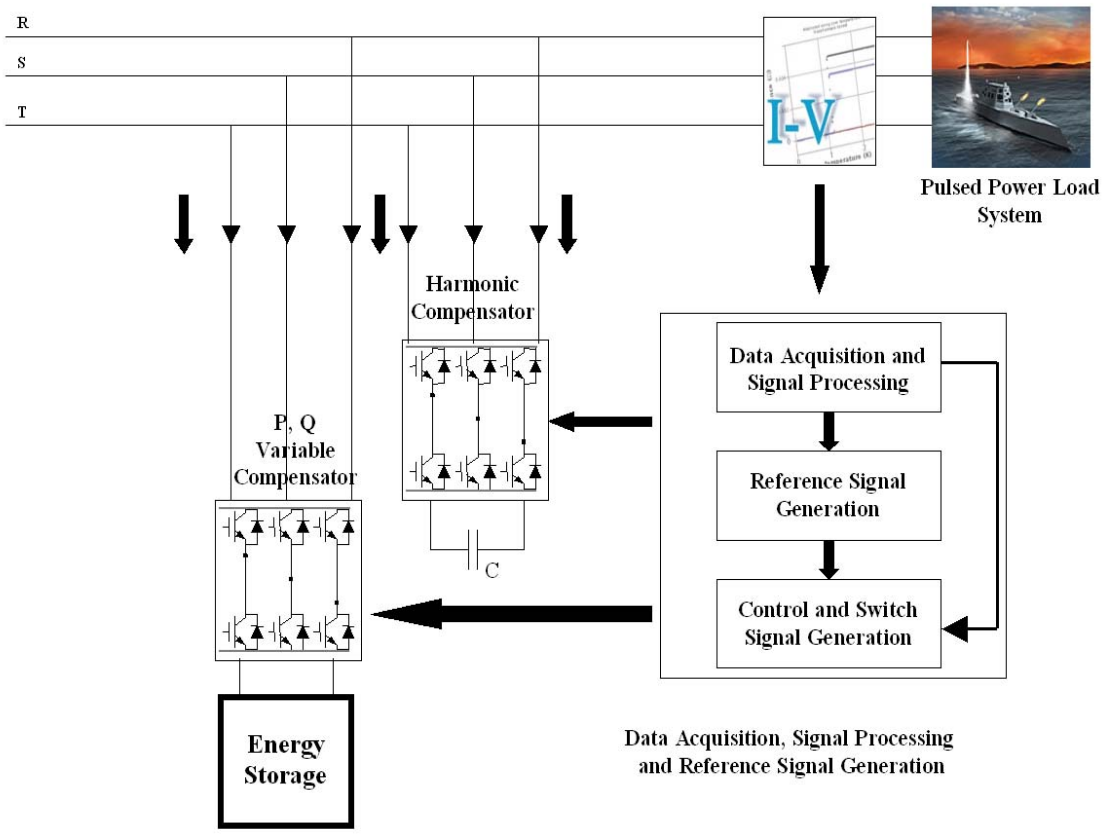

Figure 4.3 Structure of Compensators for Pulsed Power Load System

In this research work, the focus is on active power variable compensation. Therefore the required energy storage capacity and the rating of the three phase converter(s) need to be known. There are many options with respect to the selection of energy storage device.

As far as the control system is concerned, the data acquisition and signal processing block makes use of the moving window discrete Fourier transformation to obtain the complex RMS value of the fundamental harmonic of voltage and current measurements. CPC Power Theory is used for the decomposition of load current signal in the Reference Signal Generation block of the converter control system. It is assumed that

all control below the Reference Signal Generation allows the converter to be seen as a controlled current source that follows the generated reference signal. Details of the converter control are beyond the scope of this thesis.

4.3 Supply Side Effects of Pulsed Power Load Systems

Consider a series RLC circuit as shown in Figure 4.4 with a source voltage $v_{do}(t)$ and zero initial capacitor voltage. R_L is the internal resistance of the inductor. The current flowing through the circuit is $i_{d0}(t)$. The source and the elements that are connected parallel to the capacitor are not a concern at this point of the derivation.

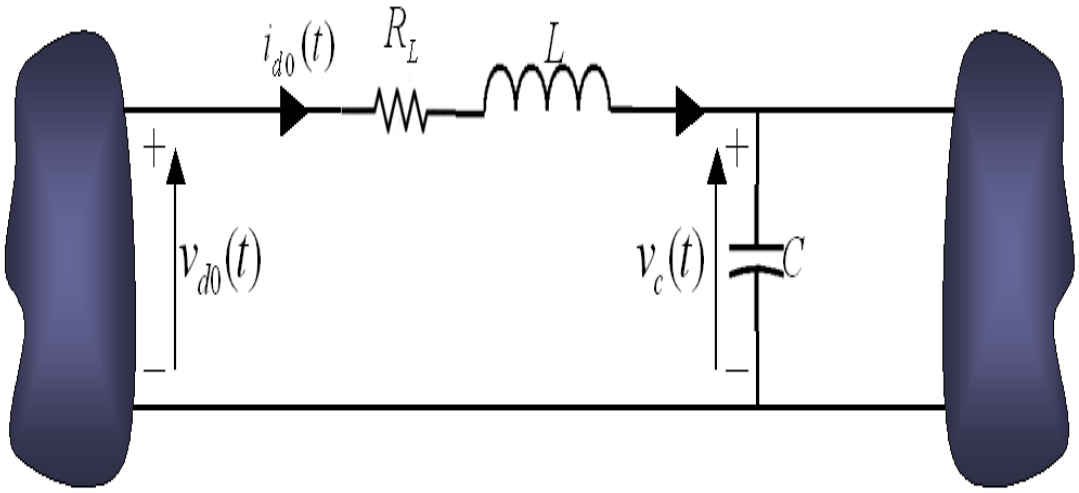

Figure 4.4 Series RLC Circuit

The loop equation for a series RLC circuit is given by,

$$L\frac{di_{d0}(t)}{dt} + R_L i_{d0}(t) + \frac{1}{C}\int_0^t i_{d0}(t)dt = v_{d0}(t) \tag{4.2}$$

differentiating Equation 4.2 on both sides with respect to t, we get

$$L\frac{d^2 i_{d0}(t)}{dt^2} + R_L \frac{di_{d0}(t)}{dt} + \frac{i_{d0}(t)}{C} = 0 \tag{4.3}$$

dividing by L on both sides we get

$$\frac{d^2 i_{d0}(t)}{dt^2} + \frac{R_L}{L}\frac{di_{d0}(t)}{dt} + \frac{i_{d0}(t)}{LC} = 0 \tag{4.4}$$

The well-known characteristic equation is derived from Equation 4.4. This derivation can be found in many circuit analysis books. The characteristic equation is given by,

$$S^2 + \frac{R_L}{L}S + \frac{1}{LC} = 0 \tag{4.5}$$

Let S_1 and S_2 be the roots of the characteristic equation and are given by,

$$S_1 = -\frac{R}{2L} + \sqrt{\left(\frac{R}{2L}\right)^2 - \left(\frac{1}{LC}\right)} \tag{4.6}$$

$$S_2 = -\frac{R}{2L} - \sqrt{\left(\frac{R}{2L}\right)^2 - \left(\frac{1}{LC}\right)} \tag{4.7}$$

In order to avoid oscillations of the DC voltage, an underdamped case is not considered in this analytical approach. The general solution for capacitor voltage in an overdamped case is given by,

$$v_c(t) = V_c(\infty) + ae^{s_1 t} + be^{s_2 t} \tag{4.8}$$

$V_c(\infty)$ - Final value of the capacitor voltage in steady state.

a, b - Constants, which are evaluated from the initial and final conditions.

The critically damped case has a different form of general solution for capacitor voltage, which is not taken into account in this derivation. But the following steps will be

the same, apart from using a different capacitor voltage equation and the roots of the characteristic equation being real and equal. From Equations 4.6 and 4.7 we can infer that the roots of the characteristic equation S_1 and S_2 are real and unequal for the overdamped case.

Let us assume the initial condition occurs at $t = 0$. At this condition the voltage equation is written as,

$$V_c(0) = V_c(\infty) + a + b \tag{4.9}$$

where, $V_c(0)$ is the initial value of the capacitor voltage.

$$a + b = V_c(0) - V_c(\infty) \tag{4.10}$$

The equation of the current through a capacitor is given by,

$$i_c(t) = C\frac{dv_c(t)}{dt} = i_{d0}(t) \tag{4.11}$$

$i_c(t)$ - Current through a capacitor.

Equation 4.11 can be related to the initial conditions i.e. $t = 0$, where $i_c(t) = 0$

$$\frac{i_c(0)}{C} = \frac{dv_c(0)}{dt} \tag{4.12}$$

$$\left.\frac{dv_c(t)}{dt}\right|_{t=0} = 0 \tag{4.13}$$

differentiating Equation 4.8 with respect to t at $t = 0$, we get

$$s_1 a + s_2 b = 0 \tag{4.14}$$

solving Equations 4.10 and Equation 4.14 we can express a and b,

$$a = \left(\frac{s_2}{s_1 - s_2}\right)\left(V_c(\infty) - V_c(0)\right) \tag{4.15}$$

$$b = \left(\frac{s_1}{s_1 - s_2}\right)\left(V_c(0) - V_c(\infty)\right) \tag{4.16}$$

$$s_1 a = -s_2 b \tag{4.17}$$

from Equation 4.11 we get,

$$i_{d0}(t) = C\left(s_1 a e^{s_1 t} + s_2 b e^{s_2 t}\right) \tag{4.18}$$

At this stage of the derivation it is required to reveal some parts of the system in Figure 4.4. As shown in Figure 4.5, the DC voltage $v_{d0}(t)$ is the output of a three-phase diode bridge and will contain ripples. The left side of the diode bridge in Figure 4.5 will be referred to as AC side and the right side will be referred to as DC side. The currents on the AC side in lines R, S and T will contain harmonics of the order n due to the presence of a six-pulse diode bridge rectifier.

Where, $n = 6k \pm 1;\ \ k = 1,2,3\ldots.$

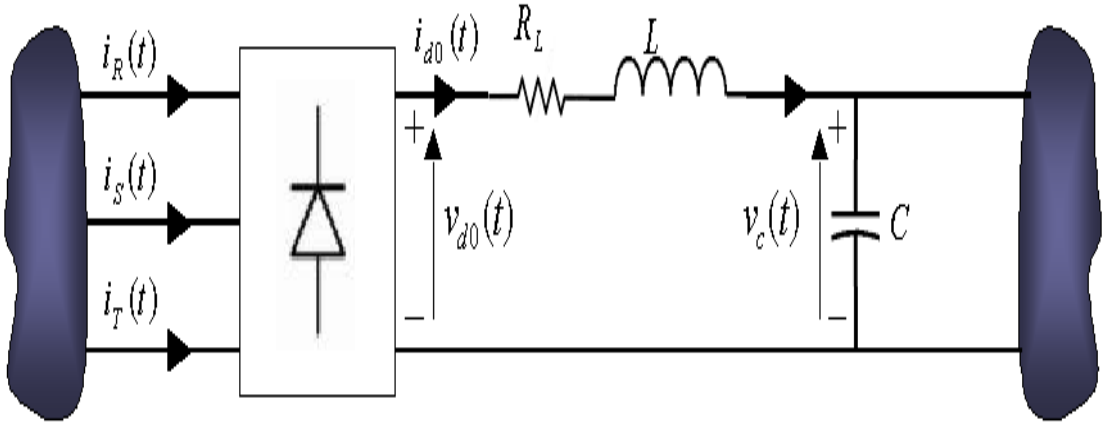

Figure 4.5 Series RLC circuit Connected to a Three-Phase Diode Bridge Rectifier

The average value of the output voltage over a cycle for a six-pulse diode bridge is expressed as,

$$V_{d0} = 6\left(\frac{1}{2\pi}\right)\int_{-\frac{\pi}{6}}^{\frac{\pi}{6}} v_{d0}(t)dt \tag{4.19}$$

V_{d0} - Average Value of the DC Output Voltage from a Six Pulse Diode Bridge Rectifier.

$$v_{d0}(t) = \sqrt{6}V_{LN}\cos\omega t d(\omega t) \tag{4.20}$$

V_{LN} - RMS value of the Line to Neutral voltage on the AC side.

$$V_{d0} = 6\left(\frac{1}{2\pi}\right)\int_{-\frac{\pi}{6}}^{\frac{\pi}{6}} \sqrt{6}V_{LN}\cos\omega t d(\omega t) \tag{4.21}$$

$$V_{d0} = \frac{3\sqrt{6}}{\pi}V_{LN} \tag{4.22}$$

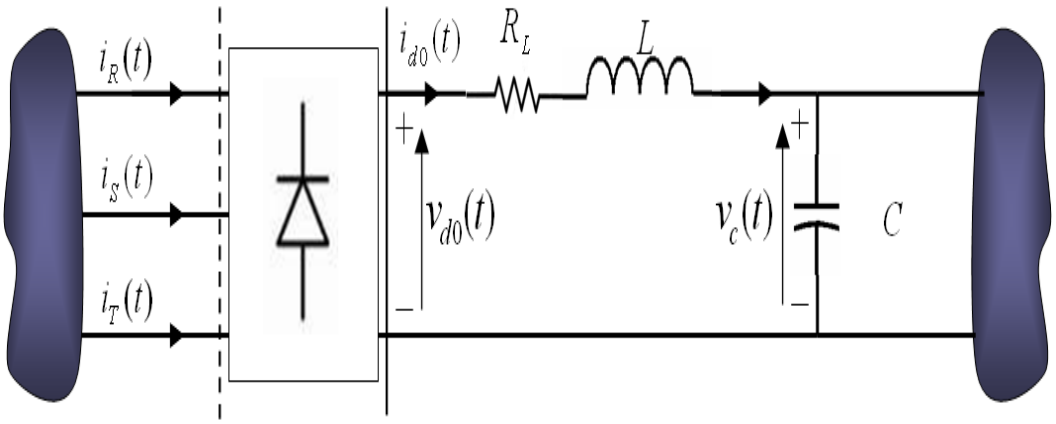

Figure 4.6 Indication of the Measurement Location in Figure 4.5

Assuming no losses in the rectifier, the energy is the same at the AC side and DC side or in other words energy is unchanged at the input and output terminals of the three-phase diode rectifier. The energy measurement is obtained from the active power over one cycle. To find the average value of the active power over one cycle, the equivalent conductance of the fundamental harmonic $\tilde{\tilde{G}}_{e1}$ (discussed in previous chapter) is to be calculated from the current and voltage values measured at the dashed line shown in Figure 4.6. These issues were discussed in the previous chapter in detail. The energy measurement at the DC side is obtained from the voltage and current value measured at the solid line.

In order to analytically determine the AC side characteristics (i.e. RMS value of the fundamental harmonic of the active current) in terms of DC side parameters, we start from the equation,

$$\tilde{\tilde{P}}_{AC} = \tilde{\tilde{P}}_{DC} \tag{4.23}$$

$\tilde{\tilde{P}}_{AC}$ - Running active power drawn by the load over one cycle of the supply voltage.

$$\tilde{\tilde{P}}_{AC} = 3V_{LN}\,\tilde{\tilde{I}}_{1a} \tag{4.24}$$

$\tilde{\tilde{I}}_{1a}$ - RMS value of the fundamental harmonic of active current on the AC side.

$$\tilde{\tilde{P}}_{DC} = V_{d0}\,\tilde{\tilde{I}}_{d0} \tag{4.25}$$

where, $\tilde{\tilde{I}}_{d0} = i_{d0}(t)$.

Due to the DC side inductor the output current ripples will be small and can be neglected. Substituting Equations 4.24 and 4.25 in Equation 4.23, we have

$$3V_{LN}\,\tilde{I}_{1a} = V_{d0}\,\tilde{I}_{d0} \tag{4.26}$$

substituting Equation 4.22 in Equation 4.26,

$$3V_{LN}\,\tilde{I}_{1a} = \frac{3\sqrt{6}V_{LN}}{\pi}\,\tilde{I}_{d0} \tag{4.27}$$

$$\tilde{I}_{1a} = \frac{\sqrt{6}}{\pi}\,\tilde{I}_{d0} \tag{4.28}$$

Substituting Equation 4.18 in Equation 4.28,

$$\tilde{I}_{1a} = \frac{\sqrt{6}}{\pi}C\left(s_1 a e^{s_1 t} + s_2 b e^{s_2 t}\right) \tag{4.29}$$

substitute $\tilde{I}_{1a}$ in Equation 4.24 we get

$$\tilde{P}_{AC} = 3V_{LN}\frac{\sqrt{6}}{\pi}C\left(s_1 a e^{s_1 t} + s_2 b e^{s_2 t}\right) \tag{4.30}$$

$$\tilde{P}_{AC} = V_{d0}C\left(s_1 a e^{s_1 t} + s_2 b e^{s_2 t}\right) \tag{4.31}$$

Equation 4.31 is the expression for average value of active power over one supply voltage cycle in terms of the DC side quantities. At this point it would be appropriate to unveil the entire power system diagram, which is shown in Figure 4.7. Due to the pulse power drawing capability of the pulsed power load system, the average active power over one cycle on the AC side will be a quantity varying with time. The details and the effects of pulsed power load system on the AC side were discussed in Section 2.3 of Chapter 2. The shape of $\tilde{P}_{AC}$ on the AC side is dependent on five parameters. They are,

1. Energy per pulse of the pulsed power load.
2. Pulse Duration.
3. Internal Resistance of the inductor.
4. Inductance.
5. Capacitance.

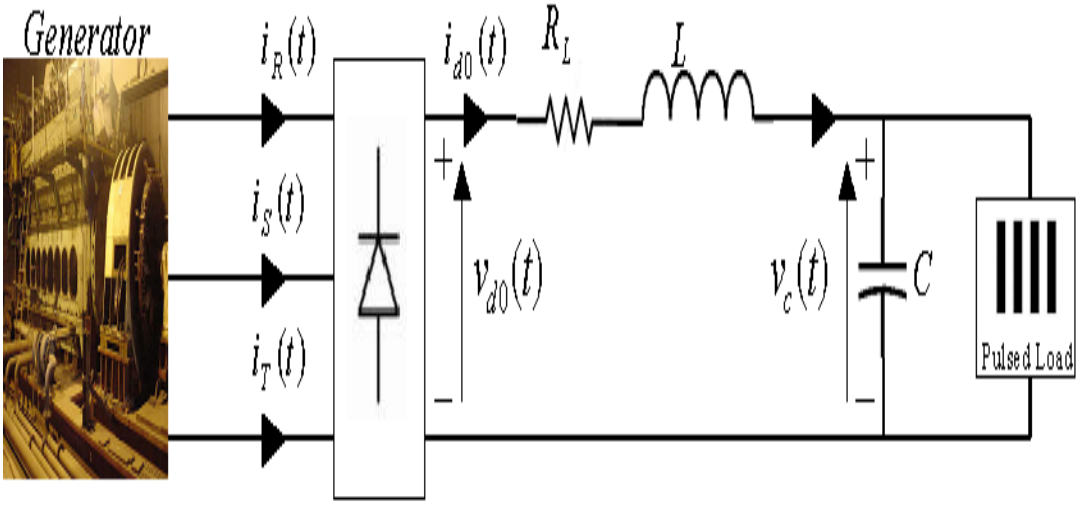

Figure 4.7 Generator supplying a Pulsed Power Load System

During the on time of the pulse, the capacitor discharges to a certain voltage $V_c(0)$ and then recharges back again to the steady state final value $V_c(\infty)$ as shown in Figure 4.8. The recharge time of the capacitor depends on the internal resistance of the inductor, inductance and capacitance. Since the capacitance used in pulsed power load applications is relatively large, the chances of capacitor voltage ripples are minimal. Hence we can equate the final value of the capacitor voltage in steady state $V_c(\infty)$ to the average value of the DC output voltage over one supply voltage cycle from a six-pulse diode bridge rectifier. So from Equation 4.22 we get,

$$V_c(\infty) = V_{d0} = \frac{3\sqrt{6}}{\pi} V_{LN} \tag{4.32}$$

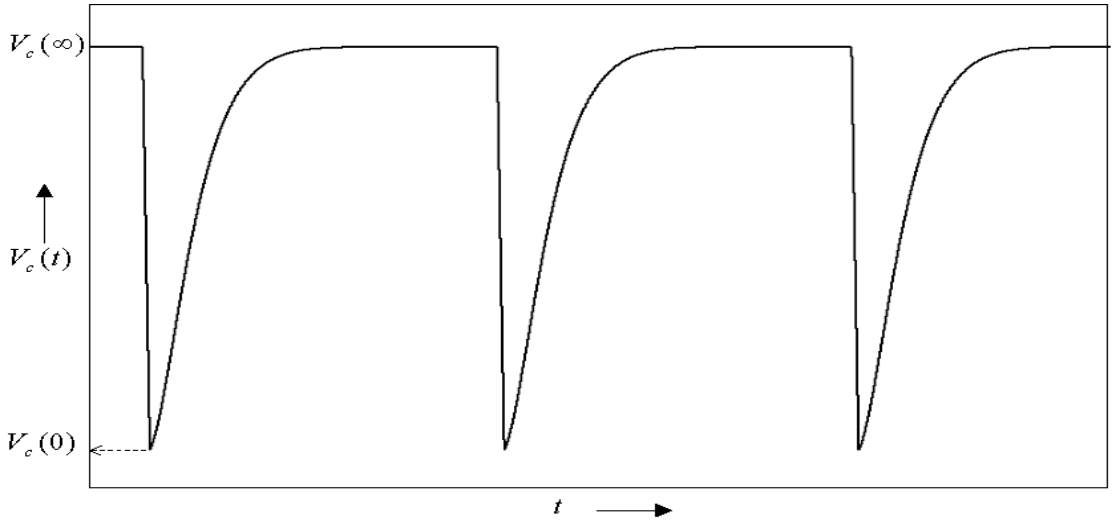

Figure 4.8 Example Plot of Capacitor Voltage during Pulsed Power Load Operation

We know that the energy per recharge E is given by,

$$E = \frac{1}{2} C\left(V_c^{\,2}(\infty) - V_c^{\,2}(0)\right) \tag{4.33}$$

rearranging Equation 4.33 we get,

$$C = \frac{2E}{\left(V_c^{\,2}(\infty) - V_c^{\,2}(0)\right)} \tag{4.34}$$

$$V_c(0) = \sqrt{V_c^{\,2}(\infty) - \frac{2E}{C}} \tag{4.35}$$

We now have all of the information required to determine the peak value of $\tilde{\tilde{P}}_{AC}$.

Each pulse causes a discharge and recharge of the capacitor voltage that makes $\tilde{\tilde{P}}_{AC}$ resemble an outcurved waveform. The duration of each waveform is equal to the recharge

time of the capacitor voltage. To find the peak value or maximum value of $\tilde{P}_{AC}$ during one discharge and recharge action of the capacitor, we differentiate $\tilde{P}_{AC}$ with respect to t and equate to zero.

$$\frac{d}{dt}(\tilde{P}_{AC}) = 0 \tag{4.36}$$

$$s_1{}^2 a e^{s_1 t} = -s_2{}^2 b e^{s_2 t} \tag{4.37}$$

substitute $t = t_P$, where, t_P is the time at which peak value occurs

$$\frac{s_1{}^2 a}{s_2{}^2 b} = -\frac{e^{s_2 t_P}}{e^{s_1 t_P}} \tag{4.38}$$

using Equation 4.17 we get

$$-\frac{s_1}{s_2} = -\frac{e^{s_2 t_P}}{e^{s_1 t_P}} \tag{4.39}$$

taking natural logarithm on both sides, we get

$$\ln\left(\frac{s_1}{s_2}\right) = \ln\left(\frac{e^{s_2 t_P}}{e^{s_1 t_P}}\right) \tag{4.40}$$

$$\ln\left(\frac{s_1}{s_2}\right) = (s_2 - s_1) t_P \tag{4.41}$$

Since the time at which peak occurs (t_P) cannot be negative in this case, we take mod on both sides,

$$|t_P| = \left|\frac{\ln\left(\frac{s_1}{s_2}\right)}{(s_2 - s_1)}\right| \tag{4.42}$$

substituting $t = t_P$ in Equation 4.29 we get, the peak value of $\tilde{\tilde{P}}_{AC}$ for a pulse ($\tilde{\tilde{P}}_{\max}$).

$$\tilde{\tilde{P}}_{\max} = V_{d0} C\left(s_1 a e^{s_1 t_P} + s_2 b e^{s_2 t_P}\right) \tag{4.43}$$

$$\|i\|_{\max} = \frac{\sqrt{6}}{\pi} C\left(s_1 a e^{s_1 t_P} + s_2 b e^{s_2 t_P}\right) \tag{4.44}$$

$\|i\|_{\max}$ - Peak of the RMS value of the fundamental harmonic of the active current drawn by the load.

The required energy per pulse can be expressed as given in Equation 4.45

$$E = \int_0^{t_r} \tilde{\tilde{P}}_{AC} dt \tag{4.45}$$

where, t_r is the recharging time of the capacitor.

4.4 Minimization of Power Loss on the DC Bus of the Pulsed Power Load System

Since the pulsed power load input currents are of the order of kA, it will lead to a considerable amount of power loss on the DC side even for small values of inductor's internal resistance. For the selection of the internal resistance of the inductor it is assumed that the power loss would be minimized.

The objective of optimization is to minimize the power loss in the DC side due to the internal resistance of the inductor (R_L). The power loss $\tilde{\tilde{P}}_{loss}$ through R_L is given by the equation,

$$\tilde{\tilde{P}}_{loss} = {i_{d0}}^2(t) R_L \tag{4.46}$$

Integrating Equation 4.46 over the recharging time (t_r) of the capacitor voltage will yield the expression E_R i.e. the loss of energy per pulse.

$$E_R = \int_0^{t_r} {i_{d0}}^2(t) R_L dt \tag{4.47}$$

substituting for $i_{d0}(t)$ and integrating with respect to t, we get

$$E_R = \frac{C^2 R_L}{2(s_1+s_2)}\left[4abs_1s_2(e^{(s_1+s_2)t_r}-1)+a^2s_1(s_1+s_2)(e^{2s_1t_r}-1)+b^2s_2(s_1+s_2)(e^{2s_2t_r}-1)\right] \tag{4.46}$$

The power loss should be minimum provided that the system is over damped and the capacitor recharges between load pulses. The constraints for the objective function are classified as follows:

- Linear Constraints:

$$R_L > 0 \tag{4.47}$$

$$L > 0 \tag{4.48}$$

- Nonlinear Inequality Constraint: (To satisfy the over damped criteria)

$$2\sqrt{\frac{L}{C}} - R_L < 0 \tag{4.49}$$

- Nonlinear Equality Constraint:

$$ae^{s_1(t_r-0.1)} + be^{s_2(t_r-0.1)} + 2 = 0 \tag{4.50}$$

The Nonlinear Equality Constraint in Equation 4.50 is to make sure that the capacitor recharges to its final value between pulses.

4.4.1 Solving the Optimization Problem

The objective function in Equation (4.46) is a nonlinear constrained multivariable function which consists of variables R_L and L. The optimization problem is solved using "fmincon" command in MATLAB Optimization toolbox. It uses sequential quadratic programming algorithm to minimize E_R in Equation 4.46. The sequential quadratic programming is similar to Newton's method for constrained optimization but is used only for unconstrained optimization. At each important iteration, the quasi-Newton updating method is used to approximate the Hessian of the Lagrangian function. This is then used to generate a quadratic programming sub problem whose solution is used to form a search direction for a line search procedure [14].

The obtained optimal values are $R_{L\,opt}$ and L_{opt}. It is obvious that the minimum E_R subject to the constraints will result in minimum $\tilde{P}_{\max}$ due to the fact that the loss is a function of current through the inductive resistance, which in turn is a function of the fundamental active current component on the AC side.

4.5 Ratings of an Energy Storage System Operating in Conjunction with the Main Generator

The energy demand of the pulsed power loads can be on the order of hundreds of MJ. Therefore an external energy storage system with a storage capacity to support the entire demand of the pulsed power load system may not be feasible in terms of size. The main generator is assumed to provide a part of the energy demand of the pulsed power load system. If this is the case, then the rest of the energy should come from the energy

storage system, which uses a control system to determine the active power to be injected into the main power system. The following derivation gives the current rating of the energy storage interface and the energy storage capacity per pulse of the energy storage device. The solution is obtained by using $R_{L\,opt}$ and L_{opt} instead of R_L and L respectively in the following expressions.

The active power supplied by the main generator is assumed to be constant and can be expressed in terms of CPC Power Theory as in Equation 4.51,

$$P_G = 3G_{e1S}V_{LN}{}^2 \tag{4.51}$$

G_{e1S} - Equivalent conductance of fundamental harmonic of the main generator.

P_G - Active power supplied by the main generator.

$$G_{e1S} = \frac{P_G}{3V_{LN}{}^2} \tag{4.52}$$

We can also express $\tilde{\tilde{P}}_{AC}$ in terms of CPC Power Theory,

$$\tilde{\tilde{P}}_{AC} = 3\tilde{\tilde{G}}_{e1}V_{LN}{}^2 \tag{4.53}$$

$\tilde{\tilde{G}}_{e1}$ - Equivalent conductance of the fundamental harmonic of the load.

$$\tilde{\tilde{G}}_{e1} = \frac{\tilde{\tilde{P}}_{AC}}{3V_{LN}{}^2} \tag{4.54}$$

$$\tilde{\tilde{G}}_{e1C} = \tilde{\tilde{G}}_{e1} - G_{e1S} \tag{4.55}$$

where, $\tilde{\tilde{G}}_{e1C}$ - Equivalent conductance of fundamental harmonic of the energy storage system.

$$\tilde{\tilde{P}}_c = 3V_{LN}{}^2 \tilde{\tilde{G}}_{e1C} \tag{4.56}$$

$\tilde{\tilde{P}}_c$ - Running Active Power to be injected by the energy storage system assuming a constant generation power.

$\tilde{\tilde{P}}_c$ is the control command issued by the controller to the energy storage system. The energy to be stored in the energy storage device for one pulse (E_{eC}) is given by,

$$E_{eC} = \int_0^{t_r} 3\tilde{\tilde{G}}_{e1C} V_{LN}{}^2 dt \tag{4.57}$$

The peak of the RMS value of the fundamental harmonic of active current injected by the energy storage device ($\|i\|_{C\max}$) is given by,

$$\|i\|_{C\max} = \frac{\tilde{\tilde{P}}_{\max} - P_G}{3V_{LN}} \tag{4.58}$$

$\|i\|_{C\max}$ - Current rating of the energy storage interface i.e. three-phase converter(s).

CHAPTER V

TEST CASE AND RESULTS

5.1 Simulation Tool to Analyze the Effects of Pulsed Power Load System Compensation

A simulation tool of the power system with the pulsed power load was developed in Matlab/Simulink. It consists of a generator, pulsed power load system, energy storage system (active and reactive power compensators), harmonic compensator, and a control system. In the power system model ideal voltage sources and ideal current sources are used to model the generator and compensators (active and reactive power compensator and harmonic compensator) respectively. The control system performs three tasks, they are: data acquisition, signal processing and reference signal generation. It uses the CPC Power Theory and current decomposition techniques, which were discussed in Chapter 3 to obtain the control command for the compensators. The control command is the currents to be injected by the ideal current sources for appropriate active, reactive and harmonic compensation. The constant active power from the generator is the input parameter for the control system.

The pulsed power load system model draws current from the supply based on the input parameters shown in the pulsed power load system block parameters in Figure 5.1. The pulsed power load system model consists of three rounds of pulses; each round

consists of 6 pulses. The current drawn by each pulse on the AC side is based on the energy profile of the pulsed power load and the change in DC bus voltage across the capacitor. The details of the modeling of the pulsed power load system were discussed in Section 4.2 of Chapter 4. The simulation calculates $R_{L\,opt}$ and L_{opt} values using the Matlab Optimization tool box for the internal resistance of the inductor and inductance, respectively, in pulsed power load charging system shown. The capacitance is calculated using Equation 4.34. The block diagram of the power system simulation model is similar to Figure 4.3.

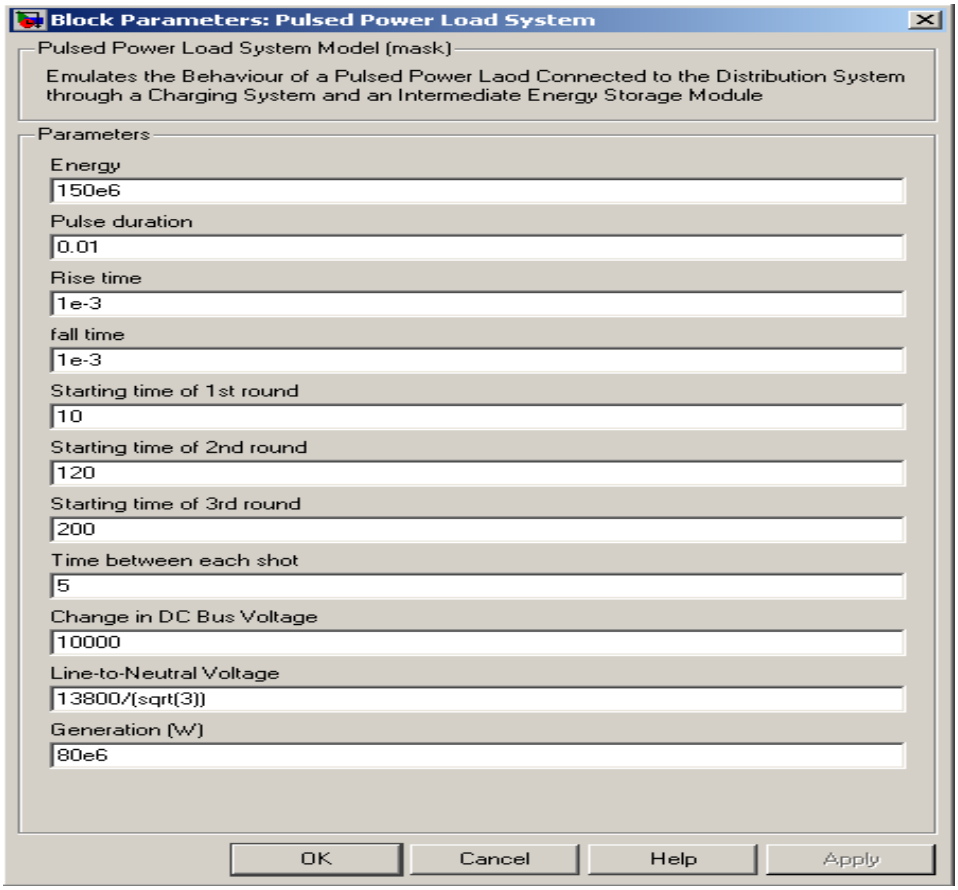

Figure 5.1 : Pulsed Power Load System Model - Input Parameters

5.2 Simulation Case Study

In order to analyze the effects of a pulsed power load system and its energy storage systems, a power system model with parameters derived from the Notional DD (X) power system outlined in Chapter 2 is simulated using the simulation tool. A pulsed power load in future electric ships may require 160 MJ of energy per pulse with a 5 second time interval between each pulse as discussed in Section 2.3 of Chapter 2. Hence if there are six pulses, then the total energy storage capacity should be 960 MJ. The allowable change in the DC bus voltage across the capacitor (IESM) is considered to be 10 KV. As per the Notional DD (X) power system discussed in Chapter 2, a constant generation power of 80 MW with generator output voltage and frequency being 13.8 KV and 60 Hz respectively are used as system parameters. It is assumed that the energy storage system is used in conjunction with the 80 MW generation active power to supply the pulsed power load system. Since we are dealing with active power compensation, there is no reactive power generation or absorption in the power system simulation model. The model is simulated using MATLAB/Simulink with the above-mentioned parameters.

- AC and DC Side Characteristics

In this case, the generation is limited to 80 MW as shown in Figure 5.3, but the peak value of the load active power shown in Figure 5.2 reaches 180 MW. Therefore the additional active power shown in Figure 5.4 is delivered by the energy storage system. The peak of the RMS value of the injected active current is 4258 A as it can be observed from Figure 5.5 and the energy storage required for operation of one pulse is 71.6 MJ. As

shown in Figure 5.6 the change in DC bus voltage is exactly 10 KV as specified in the input of the pulsed power load system model. As the drop in DC bus voltage across the capacitor (IESM) increases the required active current increases and vice versa due to fact that the capacitance is inversely proportional to the drop in the DC bus voltage across the capacitor. The input current of the pulsed power load on the DC side is shown in Figure 5.7.

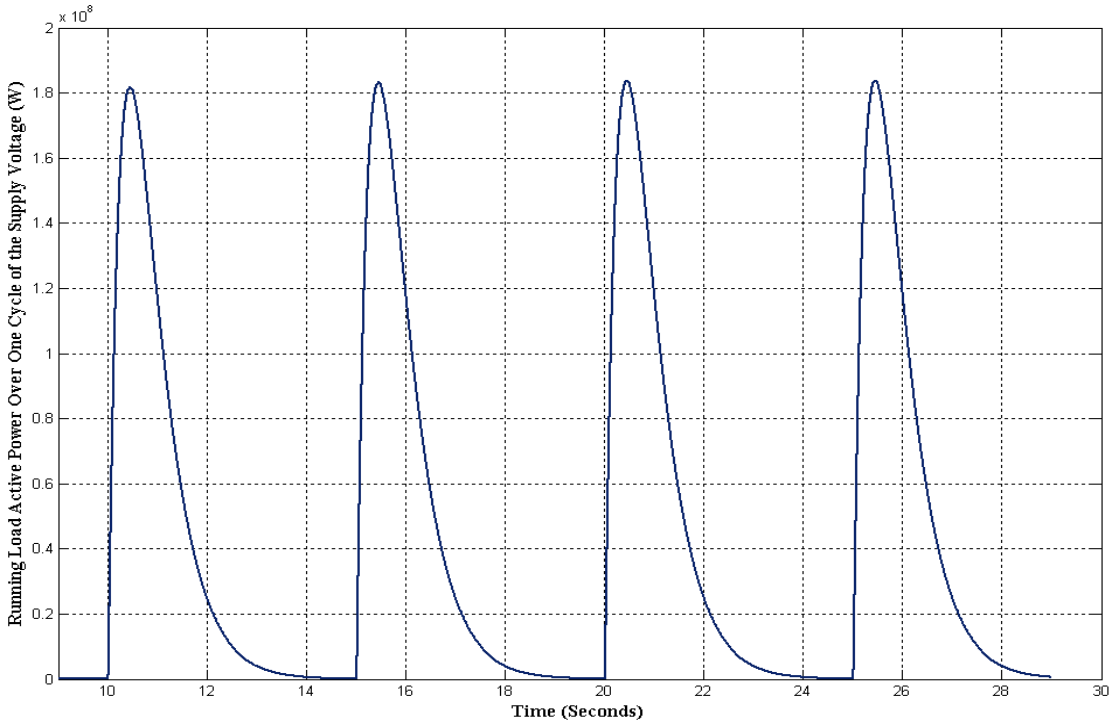

Figure 5.2 Running Load Active Power Over One Cycle of the Supply Voltage

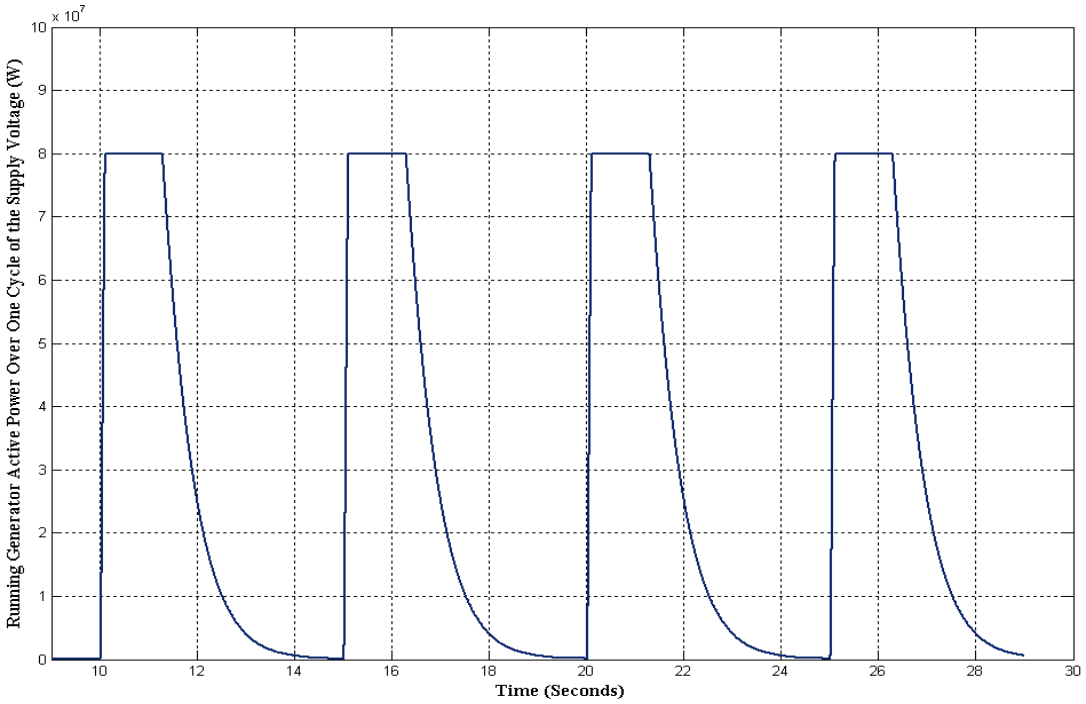

Figure 5.3 : Running Generator Active Power Over One Cycle of the Supply Voltage

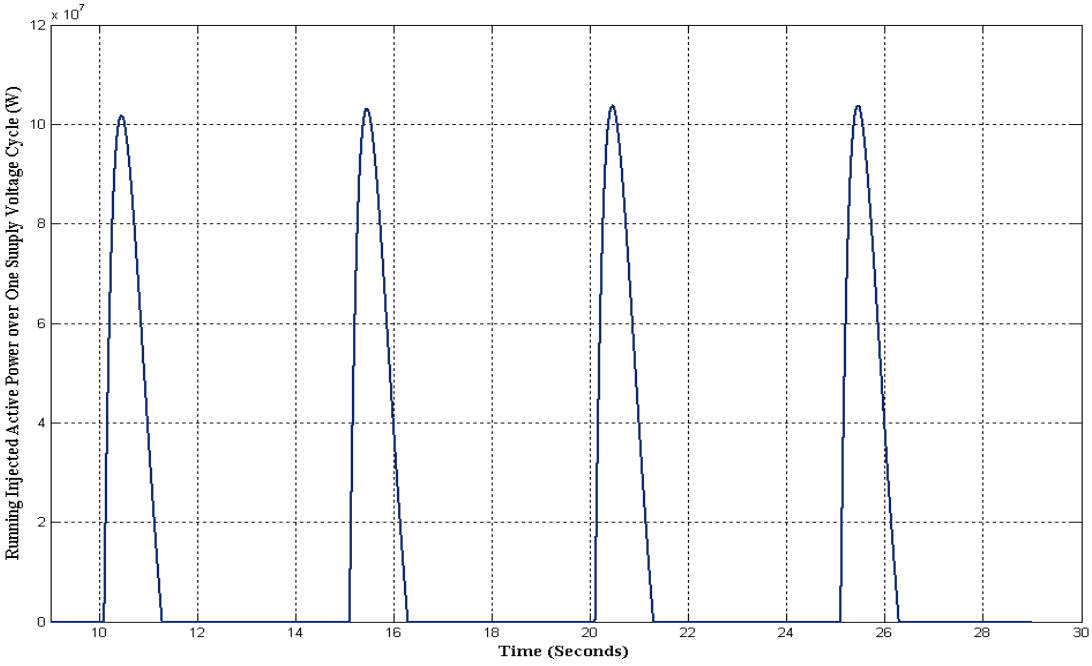

Figure 5.4 : Running Injected Active Power Over One Cycle of the Supply Voltage

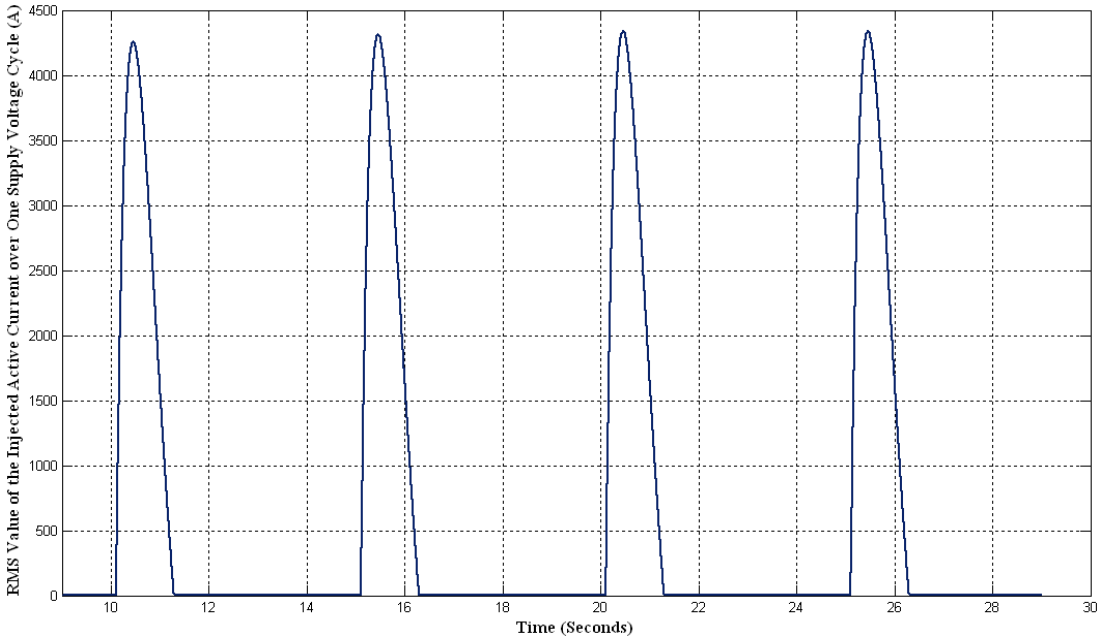

Figure 5.5 : RMS Value of the Injected Active Current Over One Cycle of the Supply Voltage

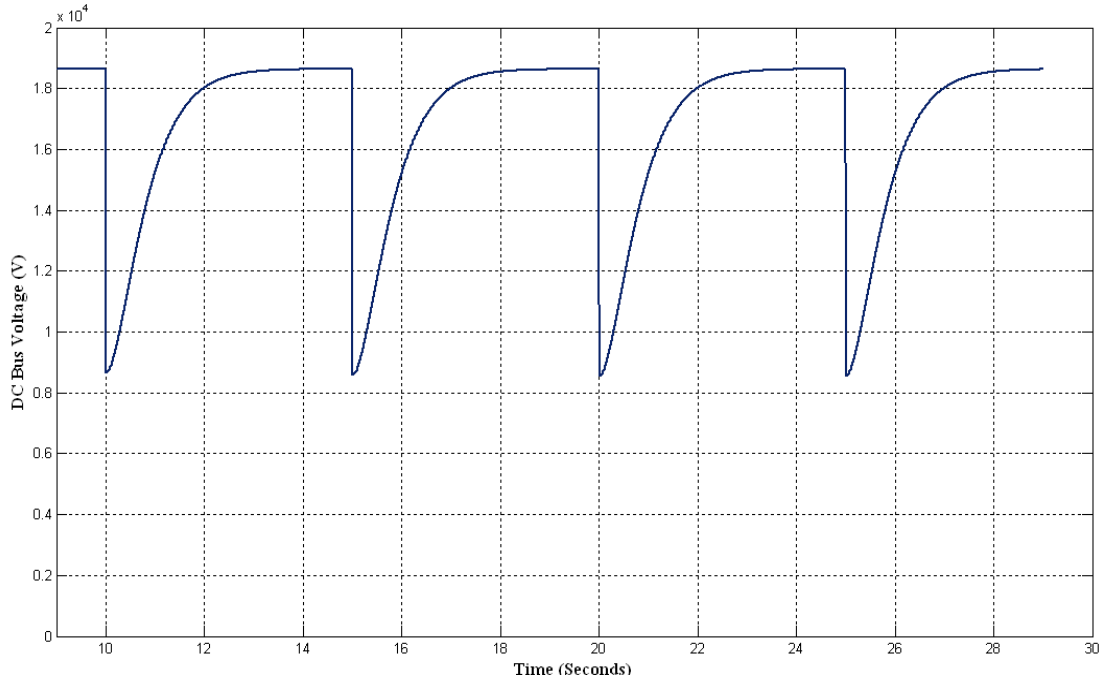

Figure 5.6 : DC Bus Voltage Across the Capacitor

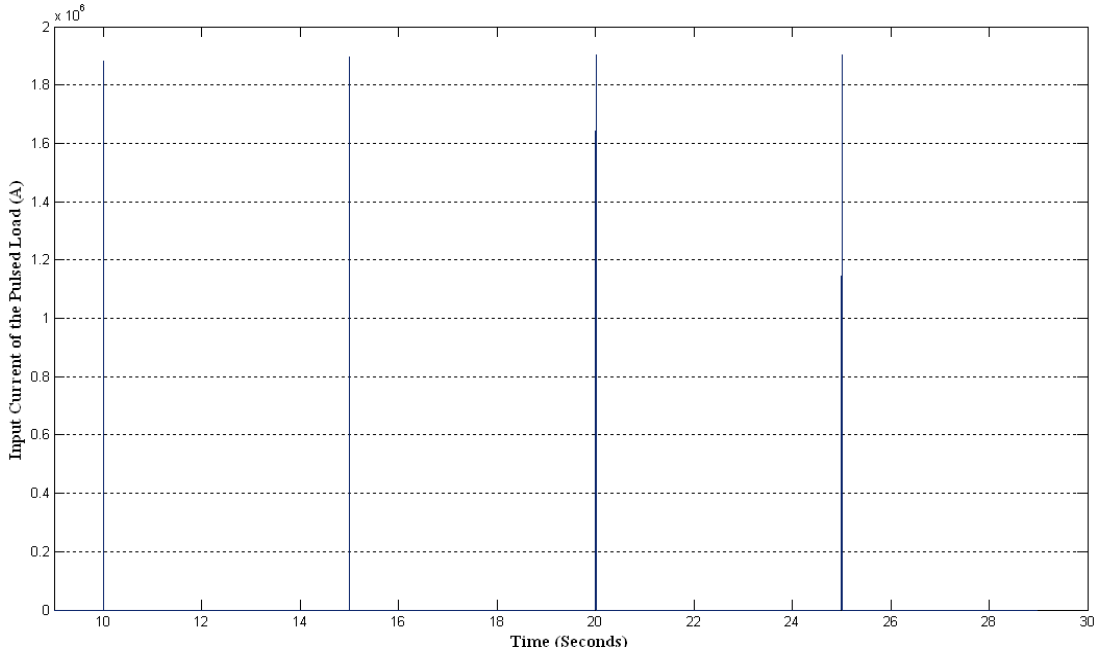

Figure 5.7 : Input Current of the Pulsed Power Load

5.3 Analytical Tool to Analyze the Effects of Pulsed Power Load System Compensation

One of the disadvantages of the simulation tool discussed in the previous Section is that, it may take a few minutes to run the simulation on a modern PC with a 2.5 GHZ processor. Using the analytical approach in Chapter 4, an analytical tool can be developed to determine the energy storage capacity per pulse and the current rating of the energy storage interface i.e. the three-phase converter(s). Figure 5.8 shows the pictorial representation of the tool used to obtain the ratings of the energy storage interface and the energy storage capacity. As shown in Figure 5.8 the required input parameters are:

1. Energy per Pulse
2. Time interval between each Pulse
3. Available generation Power

4. Allowable Change in DC bus voltage

The tool uses the Matlab optimization tool box to obtain the optimal charging circuit values as discussed in Section 4.4 of Chapter 4. It outputs the value of the required energy storage per pulse using Equation 4.57 and the peak of the RMS value of the active current injected by the energy storage system using the Equation 4.58, which gives the rating of the energy storage interface. These two values are calculated using this analytical tool for the case discussed in the previous Section and compared with the values obtained from the simulation tool. The comparison is shown in Table 5.1 and it is evident that the results generated by the analytical tool closely matched the simulation results.

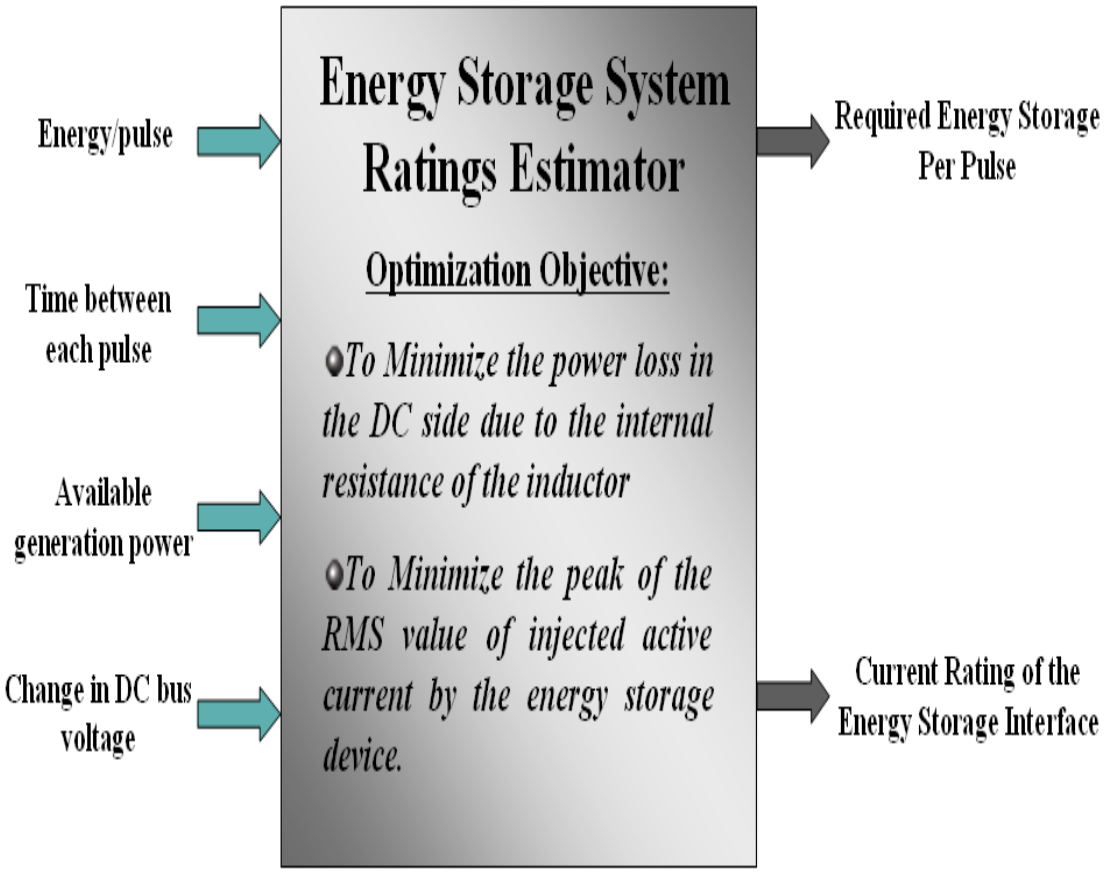

Figure 5.8 Pictorial Representation of the Analytical Tool used to Estimate the Ratings of the Energy Storage System

Table 5.1 Comparison Between Simulation Tool and Analytical tool

	Simulation Tool	Analytical Tool
Required Energy Storage Per Pulse for 80 MW Generation	71.6 MJ	71.5 MJ
Current Rating of the Energy Storage Interface	4258 A	4243 A

5.4 Numerical Tests

In future electric ships the total generation power may range from 80 MW to 100 MW. The energy required for large pulsed power loads may range from 100 MJ to 200 MJ per pulse with the time interval between each pulse being in the range between 1 to 10 seconds. Therefore it will be useful to obtain the information on the energy storage interface for a wide range of pulsed power load profiles.

An algorithm is developed in Matlab using the analytical tool to obtain the optimal current ratings of the energy storage interface for pulsed power load systems with a time interval between each pulse ranging from 1 to 8 seconds in steps of 0.5 seconds. The input parameters to the algorithm are: available active power generation, allowable change in DC bus voltage across the capacitor and the energy per pulse of the pulse power load. Two surface plots are obtained using the data from the algorithm assuming a generation power of 80 MW and allowable change in DC bus voltage of 5 KV and 10 KV. Current Ratings of the energy storage interface and the energy storage capacity for Pulsed power loads with energy from 100 MJ/Pulse to 200 MJ/Pulse in the steps of 100 MJ are calculated using this algorithm. The data tables used for the surface plots are shown in the Appendix Section. The surface plots with the Current Rating of the Energy Storage Interface for two cases are shown in Figures 5.9 and 5.10.

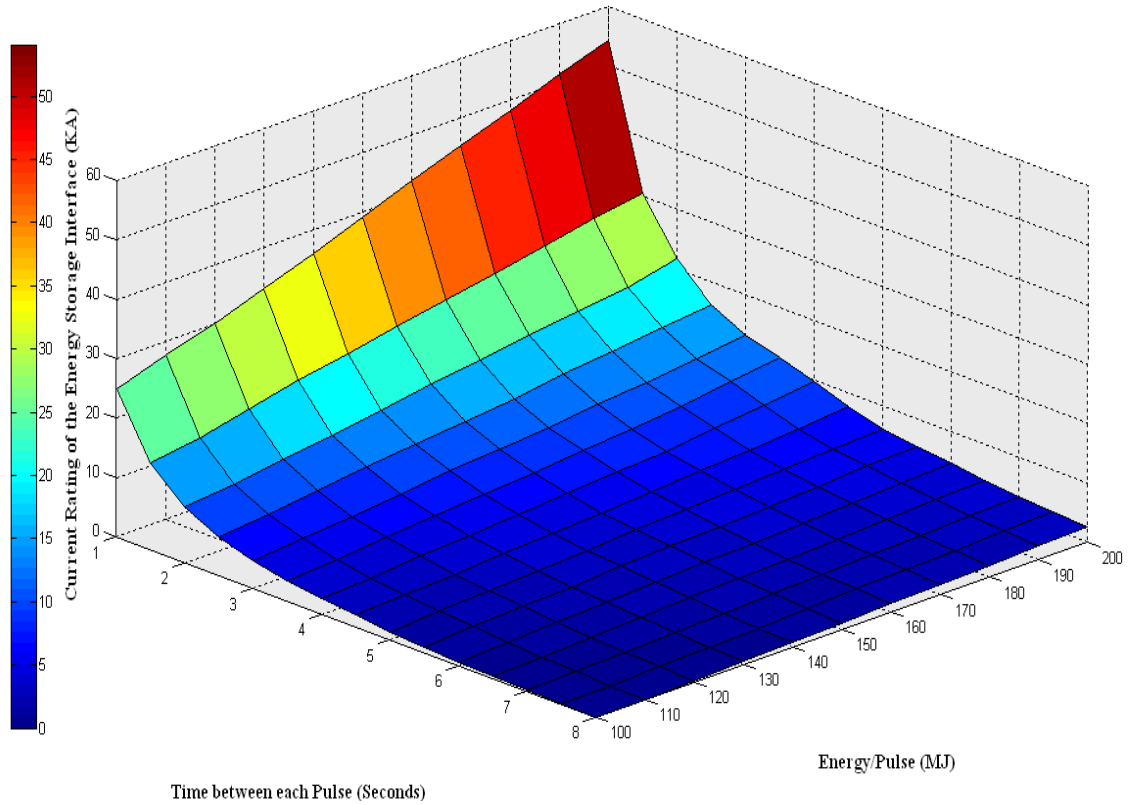

Figure 5.9 : Current Ratings of Energy Storage Interface for 80 MW Generation Power and 10 kV Change in DC Bus Voltage.

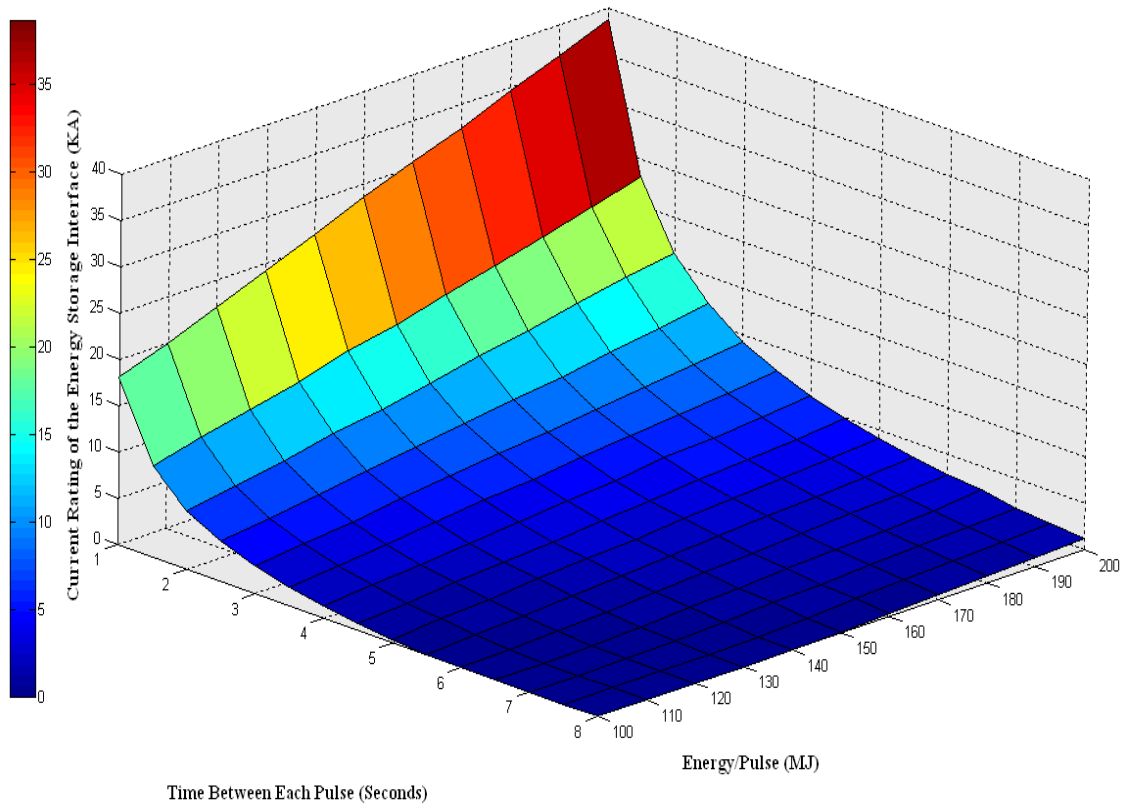

Figure 5.10 : Current Rating of Energy Storage Interface for 80 MW Generation Power and 5 kV Change in DC Bus Voltage.

CHAPTER VI

CONCLUSIONS

An approach for finding the time varying RMS value of active current in AC systems supplying pulsed power loads was proposed. Using the proposed approach, a tool was developed that determines the current ratings of an energy storage interface to the main AC system (three-phase converter) and the required energy storage capacity of the energy storage device as a function of load and supply parameters for a given pulsed power load profile, generator active power and the pulsed power load charging system parameters. The tool demonstrates that it is possible to obtain the fundamental energy storage system requirements for any pulsed power load system profile.

The results obtained using the developed tool were validated with the results obtained from the simulation model of the generator supplying a pulsed power load in conjunction with an energy storage system. The simulation model uses the Moving-Window Discrete Fourier Transform for obtaining the complex RMS value of the fundamental harmonic of load current and Current's Physical Components power theory to generate the reference signal for the active, reactive and harmonic compensators. The simulation model demonstrates that it is feasible to characterize the load current of a pulsed power load system, which is aperiodic due to the time variance of the load parameters into its physical components using Current's Physical Components power theory. Since the active, reactive and distortion powers of a pulsed power load system

vary with time and the energy transfer is associated only with the fundamental frequency, it was shown that the Moving-Window Discrete Fourier transform can be used effectively to detect the change in load current at the fundamental frequency.

Although the techniques and methods were focused on a particular structure of the pulsed power load system, the signal processing and reference signal generation techniques used in this thesis can be applied to any type of load, with semi-periodic currents. Therefore the approach proposed in this thesis may be applied to determine the energy storage interface current rating and the energy storage device capacity for any type of pulsed power load system connected to an AC distribution system. This approach can be extended to develop the mathematical expressions required to determine the fundamental energy storage system requirements for other types of pulsed power load system configuration. The slope of the RMS value of the active current injected by the energy storage system, which was obtained using the analytical approach, can be used to determine the type of the energy storage medium to be used in the energy storage system for future work.

REFERENCES

[1] An Integrated Electric Power System: the NEXT STEP [Online] http://www.globalsecurity.org/military/library/report/2000/power_system.htm

[2] Electric Ship Propulsion Systems [Online] http://www.iee.org/oncomms/sector/power/Articles/Download/5BCA2174-828B-41CE-8739E3940DC1FF3A

[3] Timothy J. McCoy, "Trends in ship electric propulsion," *Proceedings of the* 2002 *IEEE Power Engineering Society Summer Meeting,* vol.1, July 2002, pp. 343-346.

[4] ONR / NSF EPNES Control Challenge Problem [Online] http://www.usna.edu/EPNES/ONR_Control_Challenge.pdf

[2] Lori N. Domaschk, Abdelhamid, Robert E. Hebner, Oscar E. Bowlin, W.B. Colson, "Coordination of Large Pulsed Loads on Future Electric Ships," *IEEE Transactions on Magnetics,* vol. 43, no. 1, January 2007, pp. 450-455.

[6] J.H. Beno and E.A. Lewis, "Managing multiple and varying energy demands by means of energy storage in combatants with integrated electric propulsion," *Presented at the Engine as a Weapon Symposium*, Bristol, UK, June 9-10, 2004.

[7] Czarnecki, L.S, "Harmonics and Power Phenomena," in *Wiley Encyclopedia of Electrical and Electronics Engineering,* New York: Wiley, 2000, pp. 195-218.

[8] Leszek S. Czarnecki, Ernest A. Mendrala, Herbert L. Ginn III, "Decomposition of Pulsed Loads Current for Hybrid Compensation," *L'Energia Elettrica – Volume 81 (2004)*

[9] Herbert L. Ginn III, "AModified Instantaneous Reactive Power Compensation Algorithm," *Electrical Power Quality and Utilization Journal,* Volume XIII, No. 1, 2007, pp. 55-57.

[10] Claude Baumann, "RFT: a simplified real-time sliding DFT algorithm," Reading, September 15 2005.

[11] L.S. Czarnecki, "Currents' Physical Components (CPC) in Circuits with Nonsinusoidal Voltages and Currents. Part 2: Three-Phase Linear Circuits," *Electrical Power Quality and Utilization Journal*, V. XXII, No. 1, 2006.

[12] Czarnecki, L.S, "Non-Periodic Currents: Their Properties, Identification and Compensation Fundamentals," *Proceedings of the 2000 IEEE Power Engineering Society Summer Meeting*, vol. 2, July 2000, pp. 971-976.

[13] Czarnecki, L.S, Shih Min Hsu, Guangda Chen, "Adaptive Balancing Compensator," *IEEE Transactions on Power Delivery*, Vol. 10, No. 3, July 1995.

[14] Mathworks Optimization Toolbox [Online] http://www.mathworks.com/access/helpdesk/help/toolbox/optim/

APPENDIX A

ENERGY STORAGE SYSTEM RATINGS (80 MW/10 kV)

Table A.1 Energy Storage Ratings for a 100 MJ Pulse (80 MW/10 kV)

Time Interval Between Each Pulse (Seconds)	Current Rating of the Energy Storage Interface (A)	Energy Storage Capacity Required Per Pulse (MJ)
1	24977	100.03
1.5	14547	85.351
2	9468.1	71.808
2.5	6409.1	58.707
3	4650.3	47.363
3.5	3454.1	38.154
4	2547.9	29.374
4.5	2076.7	24.010
5	1368.5	15.597
5.5	924.97	9.8912
6	589.70	5.6057
6.5	265.08	1.8066
7	110.38	0.5233
7.5	0	0
8	0	0

Table A.2 Energy Storage Ratings for a 110 MJ Pulse (80 MW/10 kV)

Time Interval Between Each Pulse (Seconds)	Current Rating of the Energy Storage Interface (A)	Energy Storage Capacity Required Per Pulse (MJ)
1	27778	112.84
1.5	15925	97.151
2	10282	82.438
2.5	7255.1	69.452
3	5536.7	58.985
3.5	4125.5	48.194
4	3155.0	38.991
4.5	2407.5	30.655
5	1870.9	23.914
5.5	1463.0	18.387
6	973.82	11.565
6.5	612.33	6.4852
7	373.30	3.3437
7.5	132.76	0.7738
8	0	0

Table A.3 Energy Storage Ratings for a 120 MJ Pulse (80 MW/10 kV)

Time Interval Between Each Pulse (Seconds)	Current Rating of the Energy Storage Interface (A)	Energy Storage Capacity Required Per Pulse (MJ)
1	30055	125.43
1.5	17873	109.85
2	11458	94.276
2.5	8436.7	81.840
3	6166.1	69.008
3.5	4876.8	55.516
4	3939.6	50.560
4.5	2933.9	39.959
5	2345.5	32.574
5.5	1874.8	26.087
6	1361.3	18.600
6.5	980.19	12.729
7	652.83	7.6879
7.5	420.06	4.2862
8	149.91	1.0094

Table A.4 Energy Storage Ratings for a 130 MJ Pulse (80 MW/10 kV)

Time Interval Between Each Pulse (Seconds)	Current Rating of the Energy Storage Interface (A)	Energy Storage Capacity Required Per Pulse (MJ)
1	32946	138.42
1.5	19643	122.46
2	12697	106.44
2.5	9405.7	93.509
3	7086.0	80.940
3.5	5545.1	69.861
4	4408.0	59.728
4.5	3494.7	50.061
5	2859.6	42.220
5.5	2187.9	33.082
6	1722.3	26.003
6.5	1372.5	20.316
7	994.79	14.040
7.5	145.33	9.8580
8	470.92	5.4162

Table A.5 Energy Storage Ratings for a 140 MJ Pulse (80 MW/10 kV)

Time Interval Between Each Pulse (Seconds)	Current Rating of the Energy Storage Interface (A)	Energy Storage Capacity Required Per Pulse (MJ)
1	36008	151.50
1.5	21175	134.80
2	13947	118.73
2.5	10279	104.98
3	8001.4	92.960
3.5	6130.6	80.226
4	4925.2	69.641
4.5	4070.2	60.630
5	3288.5	51.277
5.5	2763.6	44.051
6	2203.3	35.760
6.5	1782.6	28.917
7	1331.0	21.179
7.5	1025.9	15.677
8	750.46	10.965

Table A.6 Energy Storage Ratings for a 150 MJ Pulse (80 MW/10 kV)

Time Interval Between Each Pulse (Seconds)	Current Rating of the Energy Storage Interface (A)	Energy Storage Capacity Required Per Pulse (MJ)
1	39052	164.63
1.5	22842	147.37
2	15272	131.26
2.5	11253	117.00
3	8806.6	104.57
3.5	6919.6	92.151
4	5602.6	81.140
4.5	4511.0	70.173
5	3840.4	62.068
5.5	3161.6	53.079
6	2655.9	45.523
6.5	2100.2	36.612
7	1682.1	29.238
7.5	1360.9	23.225
8	1062.1	17.482

Table A.7 Energy Storage Ratings for a 160 MJ Pulse (80 MW/10 kV)

Time Interval Between Each Pulse (Seconds)	Current Rating of the Energy Storage Interface (A)	Energy Storage Capacity Required Per Pulse (MJ)
1	42218	178.48
1.5	24514	161.17
2	16406	143.49
2.5	12129	128.80
3	9454.2	115.53
3.5	7739.4	104.36
4	6210.2	92.248
4.5	5069.9	81.120
5	4242.4	71.498
5.5	3417.7	61.348
6	2889.8	52.595
6.5	2407.1	44.582
7	2040.7	37.962
7.5	1738.2	32.173
8	1352.5	24.611

Table A.8 Energy Storage Ratings for a 170 MJ Pulse (80 MW/10 kV)

Time Interval Between Each Pulse (Seconds)	Current Rating of the Energy Storage Interface (A)	Energy Storage Capacity Required Per Pulse (MJ)
1	45277	190.91
1.5	25974	172.68
2	17657	156.04
2.5	13225	141.38
3	10330	127.82
3.5	8318.9	115.28
4	6796.2	103.37
4.5	5766.3	93.450
5	4768.3	82.507
5.5	3971.9	72.306
6	3305.3	62.585
6.5	2801.7	54.326
7	2383.9	46.850
7.5	1945.1	38.513
8	1648.3	32.414

Table A.9 Energy Storage Ratings for a 180 MJ Pulse (80 MW/10 kV)

Time Interval Between Each Pulse (Seconds)	Current Rating of the Energy Storage Interface (A)	Energy Storage Capacity Required Per Pulse (MJ)
1	48173	204.13
1.5	27511	185.33
2	18711	168.30
2.5	14072	153.32
3	11119	139.74
3.5	9296.1	128.42
4	7784.2	117.34
4.5	6071.6	102.25
5	5140.6	92.133
5.5	4383.2	82.405
6	3734.1	73.024
6.5	3176.1	64.276
7	2668.8	55.118
7.5	2273.1	47.482
8	1901.3	39.849

Table A.10 Energy Storage Ratings for a 190 MJ Pulse (80 MW/10 kV)

Time Interval Between Each Pulse (Seconds)	Current Rating of the Energy Storage Interface (A)	Energy Storage Capacity Required Per Pulse (MJ)
1	51370	217.22
1.5	29272	198.29
2	19868	180.79
2.5	15156	166.02
3	12041	152.29
3.5	10514	142.71
4	8679.2	130.48
4.5	6684.5	114.46
5	5613.2	102.99
5.5	4956.9	94.561
6	4127.8	83.213
6.5	3577.3	74.455
7	2997.1	64.439
7.5	2610.4	56.960
8	2236.2	49.292

Table A.11 Energy Storage Ratings for a 200 MJ Pulse (80 MW/10 kV)

Time Interval Between Each Pulse (Seconds)	Current Rating of the Energy Storage Interface (A)	Energy Storage Capacity Required Per Pulse (MJ)
1	54092	230.52
1.5	30491	211.00
2	21723	194.53
2.5	16106	178.36
3	13200	166.18
3.5	11561	156.36
4	9724.0	144.28
4.5	7632.0	128.97
5	6107.2	114.28
5.5	5259.2	103.84
6	4527.6	93.696
6.5	3914.2	84.136
7	3327.6	75.012
7.5	2863.5	65.848
8	2473.9	58.164

APPENDIX B

ENERGY STORAGE SYSTEM RATINGS (80 MW/5 kV)

Table B.1 Energy Storage Ratings for a 100 MJ Pulse (80 MW/5 kV)

Time Interval Between Each Pulse (Seconds)	Current Rating of the Energy Storage Interface (A)	Energy Storage Capacity Required Per Pulse (MJ)
1	18053	77.675
1.5	9777.8	61.956
2	6263.1	49.003
2.5	4313.7	38.182
3	2939.1	28.146
3.5	2013.7	19.792
4	1333.9	12.797
4.5	834.36	7.3451
5	366.57	2.5103
5.5	20.825	0.0390
6	0	0
6.5	0	0
7	0	0
7.5	0	0
8	0	0

Table B.2 Energy Storage Ratings for a 110 MJ Pulse (80 MW/5 kV)

Time Interval Between Each Pulse (Seconds)	Current Rating of the Energy Storage Interface (A)	Energy Storage Capacity Required Per Pulse (MJ)
1	19901	88.102
1.5	11133	72.158
2	7214.8	58.487
2.5	4982.1	46.586
3	3577.6	36.459
3.5	2580.9	27.556
4	1806.5	19.499
4.5	1197.1	12.463
5	791.29	7.5597
5.5	356.52	2.6571
6	69.263	0.0253
6.5	0	0
7	0	0
7.5	0	0
8	0	0

Table B.3 Energy Storage Ratings for a 120 MJ Pulse (80 MW/5 kV)

Time Interval Between Each Pulse (Seconds)	Current Rating of the Energy Storage Interface (A)	Energy Storage Capacity Required Per Pulse (MJ)
1	22050	98.761
1.5	12324	82.129
2	8158.5	68.149
2.5	5726.3	55.684
3	4155.0	44.683
3.5	3073.5	35.110
4	2257.3	26.557
4.5	1617.5	18.964
5	1107.7	12.421
5.5	694.09	7.0189
6	350.50	2.8336
6.5	44.797	0.0145
7	0	0
7.5	0	0
8	0	0

Table B.4 Energy Storage Ratings for a 130 MJ Pulse (80 MW/5 kV)

Time Interval Between Each Pulse (Seconds)	Current Rating of the Energy Storage Interface (A)	Energy Storage Capacity Required Per Pulse (MJ)
1	24198	109.81
1.5	13525	92.284
2	9207.9	78.323
2.5	6479.2	65.055
3	4846.0	53.973
3.5	3612.6	43.443
4	2735.1	34.353
4.5	2033.6	25.994
5	1535.0	19.380
5.5	1024.2	12.281
6	639.58	6.8548
6.5	348.66	3.0476
7	81.148	0.0378
7.5	0	0
8	0	0

Table B.5 Energy Storage Ratings for a 140 MJ Pulse (80 MW/5 kV)

Time Interval Between Each Pulse (Seconds)	Current Rating of the Energy Storage Interface (A)	Energy Storage Capacity Required Per Pulse (MJ)
1	26293	120.43
1.5	15007	103.04
2	10082	88.048
2.5	7328.5	75.051
3	5481.9	63.099
3.5	4231.0	52.693
4	3179.1	42.166
4.5	2423.1	33.159
5	1884.7	25.901
5.5	1408.2	19.005
6	951.95	12.124
6.5	631.30	7.2496
7	383.12	3.2723
7.5	78.702	0.0389
8	0	0

Table B.6 Energy Storage Ratings for a 150 MJ Pulse (80 MW/5 kV)

Time Interval Between Each Pulse (Seconds)	Current Rating of the Energy Storage Interface (A)	Energy Storage Capacity Required Per Pulse (MJ)
1	28515	131.36
1.5	16147	113.27
2	11037	98.191
2.5	8047.6	84.583
3	6158.7	72.661
3.5	4681.1	60.832
4	3684.7	50.878
4.5	2850.4	41.135
5	2218.5	32.665
5.5	1687.9	24.815
6	1279.2	18.324
6.5	901.99	12.161
7	666.62	8.3034
7.5	348.05	3.5048
8	157.36	1.1384

Table B.7 Energy Storage Ratings for a 160 MJ Pulse (80 MW/5 kV)

Time Interval Between Each Pulse (Seconds)	Current Rating of the Energy Storage Interface (A)	Energy Storage Capacity Required Per Pulse (MJ)
1	30511	142.18
1.5	17549	124.03
2	12256	109.08
2.5	8868.8	94.672
3	6728.1	81.749
3.5	5227.2	69.954
4	4091.9	58.714
4.5	3274.8	49.376
5	2604.5	40.454
5.5	2046.5	32.198
6	1566.9	24.464
6.5	1247.2	18.956
7	871.18	12.429
7.5	604.09	7.8206
8	344.27	3.6833

Table B.8 Energy Storage Ratings for a 170 MJ Pulse (80 MW/5 kV)

Time Interval Between Each Pulse (Seconds)	Current Rating of the Energy Storage Interface (A)	Energy Storage Capacity Required Per Pulse (MJ)
1	32388	153.12
1.5	18852	134.58
2	13083	119.01
2.5	9532.9	104.25
3	7357.0	91.360
3.5	5757.0	79.128
4	4860.4	70.336
4.5	3685.8	57.725
5	2963.2	48.218
5.5	2400.4	39.854
6	1898.8	31.173
6.5	1490.2	24.603
7	1126.1	17.948
7.5	829.16	12.424
8	563.60	7.5976

Table B.9 Energy Storage Ratings for a 180 MJ Pulse (80 MW/5 kV)

Time Interval Between Each Pulse (Seconds)	Current Rating of the Energy Storage Interface (A)	Energy Storage Capacity Required Per Pulse (MJ)
1	34672	163.94
1.5	20136	145.35
2	14262	129.93
2.5	10387	114.65
3	7948.5	100.86
3.5	6320.4	88.669
4	5061.0	77.012
4.5	4109.5	66.407
5	3360.5	56.702
5.5	2715.0	47.275
6	2237.2	39.465
6.5	1748.1	30.891
7	1397.4	24.276
7.5	1061.9	17.754
8	800.35	12.592

Table B.10 Energy Storage Ratings for a 190 MJ Pulse (80 MW/5 kV)

Time Interval Between Each Pulse (Seconds)	Current Rating of the Energy Storage Interface (A)	Energy Storage Capacity Required Per Pulse (MJ)
1	36544	174.87
1.5	21586	156.00
2	15309	140.49
2.5	11124	124.71
3	8606.3	110.87
3.5	6818.9	97.906
4	5530.9	86.202
4.5	4508.8	75.060
5	3688.8	64.587
5.5	3052.9	55.280
6	2507.6	46.438
6.5	2053.0	38.347
7	1642.6	30.551
7.5	1338.7	24.411
8	1019.5	17.852

Table B.11 Energy Storage Ratings for a 200 MJ Pulse (80 MW/5 kV)

Time Interval Between Each Pulse (Seconds)	Current Rating of the Energy Storage Interface (A)	Energy Storage Capacity Required Per Pulse (MJ)
1	38700	186.10
1.5	23064	167.08
2	16137	150.07
2.5	12041	135.45
3	9259.8	120.91
3.5	7355.2	107.54
4	5997.8	95.474
4.5	4925.6	84.021
5	4079.3	73.421
5.5	3401.1	63.656
6	2816.4	54.278
6.5	2512.9	48.652
7	1906.4	37.523
7.5	1592.7	31.063
8	1238.0	23.571